

Detection and phenomenology of cosmic neutrinos

Antoine Kouchner,^{a,*} Alessandro Armando Vigliano^{b,c} and Mathieu Lamoureux^d

^a*Université Paris Cité, CNRS, Astroparticule et Cosmologie, F-75013 Paris, France*

^b*Department of Mathematical, Computer and Physical Sciences, University of Udine, Udine, Italy*

^c*Istituto Nazionale di Fisica Nucleare, Sezione di Trieste, Trieste, Italy*

^d*Centre for Cosmology, Particle Physics and Phenomenology, Université Catholique de Louvain, Louvain-la-Neuve, Belgium*

E-mail: kouchner@apc.univ-paris7.fr, alessandro.armando.vigliano@ts.infn.it,
mathieu.lamoureux@uclouvain.be

Abstract: These lecture notes relate to the course on “Detection and phenomenology of cosmic neutrinos” held at the second training school on “Quantum Gravity phenomenology in the Multi-Messenger Approach” (COST Action CA 18108). The notes explore neutrino astronomy, covering its development, scientific motivations, and current achievements. We start with an introduction and historical context, delving then into detection techniques, and current telescopes. We conclude with some selected recent results in the field.

Second Training School of COST Action CA18108 “Quantum gravity phenomenology in the multi-messenger approach”

3–10 Sept 2022

Faculty of Physics, Belgrade (Serbia),

*Speaker

Contents

1 Introduction	3
1.1 Today's picture	3
1.2 Historical aspects	3
1.2.1 The origins	3
1.2.2 First observations	5
1.2.3 Initial "crises"	6
1.2.4 Different neutrino flavors	8
1.2.5 Neutrino interactions	8
2 Neutrino Astronomy	9
2.1 Scientific motivations	9
2.2 Historical aspects	10
2.2.1 First ideas	10
2.2.2 Detection of solar neutrinos	11
2.3 Oscillation detour	12
2.4 Cosmic neutrino sources	15
2.4.1 Extra-galactic sources	15
2.4.2 Galactic sources	17
3 Neutrino Telescopes	17
3.1 Detection principle	17
3.2 Past and current telescopes	23
4 Selected Results	25
4.1 Diffuse Flux	25
4.2 Search for point sources	27
4.3 Multi-messenger search	30
4.3.1 Neutrino follow-up of other alerts	30
4.4 Follow-up of neutrino alerts	30
5 Future Prospects	32

1. Introduction

1.1 Today's picture

Sixty-seven years after their discovery, neutrinos remain the most mysterious of the fermions. Neutrinos are unique fermions with a zero electric charge and with masses whose lightness in comparison to other particles remains unexplained. Initially, they were assumed to be massless, but subsequent observations of neutrino oscillations revealed the necessity of massive neutrinos. There are three neutrino flavors associated with the corresponding charged leptons: electron neutrino ν_e , muon neutrino ν_μ , and tau neutrino ν_τ . There is a possibility of additional sterile neutrinos, which do not interact with matter.

Neutrinos are often considered evidence of physics beyond the standard model as their non-zero masses are not predicted by the theory, leading to fundamental questions about the origin of their mass and whether they are Dirac or Majorana particles. The Majorana nature implies that they are their own antiparticles. Dedicated experiments are currently looking for neutrinoless double beta decays that would be a clear signature of the Majorana nature of neutrinos [1].

Analogously to quark mixing, neutrino mass eigenstates differ from flavor eigenstates, as characterized by the PMNS (Pontecorvo–Maki–Nakagawa–Sakata) matrix (Figure 1a). In addition to three mixing angles (Θ_{13} , Θ_{23} , and Θ_{12}), the matrix contains one CP violation phase δ_{CP} that may play a key role in the generation of the matter-antimatter asymmetry in the early Universe [2]. The absolute neutrino masses currently remain uncertain, as only the differences in the squared masses (appearing in neutrino oscillation probabilities) are known, but direct mass measurement experiments, as well as indirect constraints from cosmology, may narrow down the limits on this absolute scale. The neutrino mass hierarchy (i.e. the ordering from the lightest to the heaviest) will be determined in the coming years by more precise measurements of oscillation probabilities.

Neutrino physics has been recognized with Nobel Prizes, both for their discoveries and the confirmation of neutrino oscillations. The history of neutrino research demonstrates the complexity of studying neutrinos due to their weak interactions, requiring large and ingenious detectors to unravel their secrets. For a review on neutrino physics, refer to the PDG [3].

1.2 Historical aspects

1.2.1 The origins

The story of the study of neutrinos can be traced back to more than a century ago, at the turn of the previous century, with the accidental discovery of radioactivity by Becquerel in 1896 and, three years later, the identification of three types of radiation (α , β , and γ “rays”) by Rutherford and Villard.

Initially, researchers, and in particular Lise Meitner, were studying the beta radioactivity and the β ray, i.e. the electron emitted by radioactive nuclei, finding a discrete spectrum. This was compatible with the interpretation that they had at the time that the atom was composed of a nucleus made of A protons and $A - Z$ electrons plus Z orbital electrons, and that beta radioactivity consisted of the emission of the inner electrons of the nucleus:

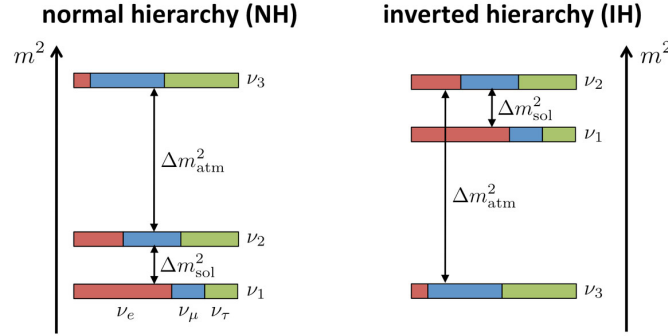
$$(A, Z) \rightarrow (A, Z - 1) + e^- \quad (1)$$

$$\begin{pmatrix} \nu_e \\ \nu_\mu \\ \nu_\tau \end{pmatrix} = \begin{pmatrix} 1 & 0 & 0 \\ 0 & c_{23} & s_{23} \\ 0 & -s_{23} & c_{23} \end{pmatrix} \cdot \begin{pmatrix} c_{13} & 0 & s_{13}e^{-i\delta_{CP}} \\ 0 & 1 & 0 \\ -s_{13}e^{i\delta_{CP}} & 0 & c_{13} \end{pmatrix} \cdot \begin{pmatrix} c_{21} & s_{12} & 0 \\ -s_{12} & c_{12} & 0 \\ 0 & 0 & 1 \end{pmatrix} \cdot \begin{pmatrix} e^{i\eta_1} & 0 & 0 \\ 0 & e^{i\eta_2} & 0 \\ 0 & 0 & 1 \end{pmatrix} \begin{pmatrix} \nu_1 \\ \nu_2 \\ \nu_3 \end{pmatrix}$$

Atmospheric
 $\theta_A \sim 45^\circ$
Reactor
 $\theta_{13} \sim 9^\circ$
Solar
 $\theta_\odot \sim 30^\circ$
Majorana

↓
CP violating phase δ_{CP}

(a) PMNS (Pontecorvo–Maki–Nakagawa–Sakata) unitary matrix.



(b) Neutrino mass hierarchy.

Figure 1: Recent picture on neutrino physics properties in terms of mixing and masses.

A few years later, in 1914, repeating the measurement of the spectrum of the beta electron with ionization chambers, Chadwick, instead of finding a mono-energetic spectrum, measured a broad spectrum with some peaks. Although, at first, Chadwick himself had rejected this result as affected by measurement errors, subsequent measurements (conducted among others by Meitner herself) confirmed this result. This finding was in apparent contradiction to the law of conservation of energy, as it appeared that energy was lost in the beta decay process, and various proposals were advanced to explain it.

On the one hand, Niels Bohr proposed that the energy is conserved only statistically, meaning that in some processes there is no conservation of the energy [4]. On the other hand, another desperate remedy was proposed by Wolfgang Pauli: there is an undetected particle that is emitted along with the electron and it carries part of the energy, i.e. the energy that is missing, so that the total of the energy represents the difference between the mass of the parent nucleus and the daughter nucleus.

This proposal had the virtue of not only predicting the correct spectrum for the beta electrons but also of solving “the wrong statistics of nitrogen and lithium” problem, i.e. the contradiction between Rutherford’s prediction of a half-integer spin for ^{14}N and ^6Li and the measured integer values. The nucleus would then be made up of protons and other neutral particles of spin 1/2. In his original letter submitted in December 1930, Pauli called this new particle the “neutron”.

As the actual neutron was discovered by Chadwick in 1932, Pauli’s hypothetical particle (yet to be observed) was later renamed “neutrino”. In 1933, Fermi introduced a theory including the neutrinos in the beta decay [5]. Fermi proposed a low energy effective theory for the β decay as a

four-fermion local interaction in which a neutron decays into a proton, an electron, and a neutrino, as in Figure 2. In addition to explaining the β decay, Fermi’s model predicted two other reactions, electron capture and inverse β decay, that could be used for the indirect detection of this elusive particle. Fermi’s theory led to the development of a full theory of weak interactions mediated by the W^\pm and Z bosons [6] (Figure 3).

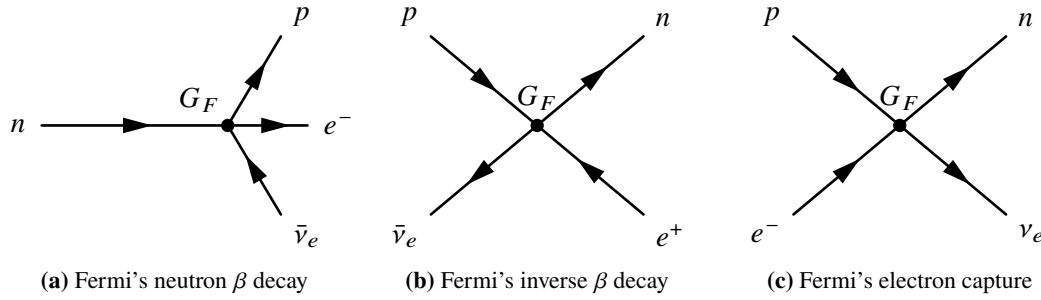


Figure 2: Feynman diagrams of Fermi’s effective theory.

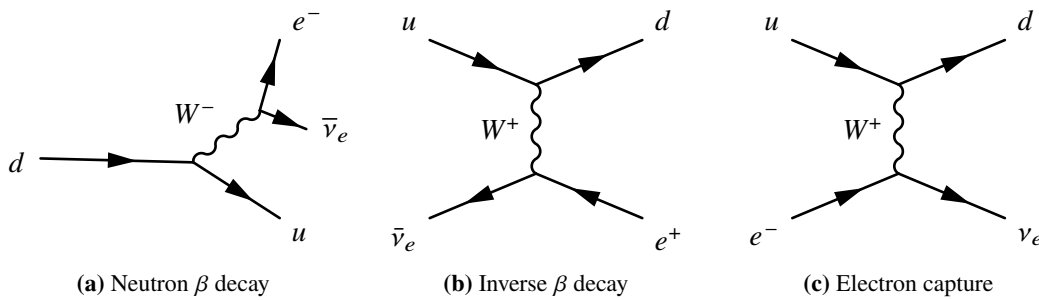


Figure 3: Feynman diagrams of weak interaction vertices, where u, d are the “up” and “down” quarks, which constitute protons and neutrons.

1.2.2 First observations

In 1953, Reines and Cowen attempted to measure the results of the inverse β decay induced by reactor neutrinos ($p + \bar{\nu}_e \rightarrow n + e^+$). This was the Hanford experiment, also known as the “Poltergeist” experiment (Figure 4a) which, using 300 liters of liquid scintillators for the detection, led to encouraging first results, but with too high background. A new improved version was subsequently attempted in 1956 close to the Savannah River reactor (the biggest reactor at the time), where 350 liters of water and Cadmium chloride CdCl_2 were used as a target for reactor neutrinos. Neutrinos interact with protons, emitting a positron (e^+) and a neutron (n). These lead to two different gamma pulses of a prompt signal from $e^+ + e^- \rightarrow \gamma + \gamma$ and a delayed signal from the absorption of the neutron by one Cadmium nucleus ($n + {}^{108}\text{Cd} \rightarrow {}^{109}\text{Cd}^* \rightarrow {}^{109}\text{Cd} + \gamma$), as illustrated on Figure 4b. This, together with a better design of the detector equipped with anti-coincidence shields, allowed a better rejection of the background due to cosmic rays, leading to the first detection of a neutrino (actually electron anti-neutrino). For this discovery, Reines was awarded the Nobel Prize in 1995 (Cowan was unfortunately dead by the time the award was issued).

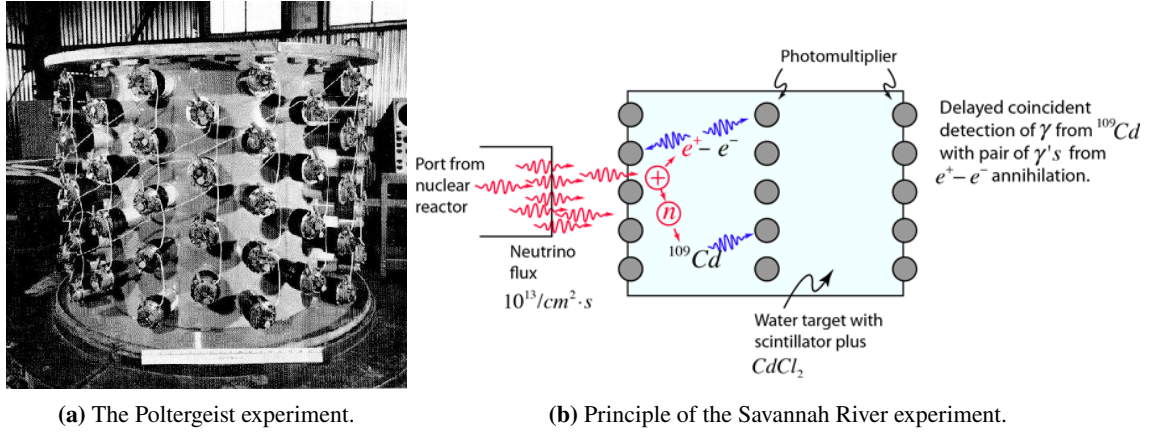


Figure 4: Illustration of the two experiments led by Cowan and Reines, leading to the first detection of neutrinos [7].

1.2.3 Initial “crises”

In 1946, Pontecorvo proposed a radiochemical method for neutrino detection, based on the observation of the decay of daughter nuclei created by neutron capture of neutrinos in some parent atoms: $\nu_e + {}_Z^AX \rightarrow {}_{Z+1}^AY + e^-$. A promising candidate reaction was proposed to be $\nu + {}_{17}^{37}\text{Cl} \rightarrow {}_{18}^{37}\text{Ar} + e^-$ for several reasons: the detector medium could be made from CCl_4 or C_2Cl_4 , cheap, non-flammable liquids, which meant that big volumes could be used; ${}^{37}\text{Ar}$ is unstable, but with a convenient half-life (~ 34.8 days), which meant that it was easy to extract and measure; the reaction has a low neutrino capture threshold $E_\nu \geq 0.814$ MeV. Two different sources of neutrinos were considered, reactor and solar neutrinos.

This detection technique was tried for the first time by Davis in 1955 at Brookhaven with 3800 liters of CCl_4 and then again at Savannah River in 1958 using 11400 liters. After an exposure of CCl_4 of 100 days, the Argon atoms were extracted and the radioactivity was measured with Geiger counters. Both attempts got negative results leading to some very strong constraints on the (anti)neutrino capture cross-section: $\sigma_\nu < 0.9 \times 10^{-45} \text{ cm}^{-2}$, which was below the predictions from interaction models.

At the time, this result was quite puzzling as it implied that neutrinos emitted along the electron by nuclear fission reactions $n \rightarrow p + e^- + \bar{\nu}_e$ can interact with free protons (Reines and Cowan results), $\bar{\nu}_e + p \rightarrow n + e^+$, but not be captured by Cl atoms (Davis results) $\bar{\nu}_e + n \rightarrow p + e^-$ and therefore neutrinos must be different from antineutrinos. A few years later, Davis attempted another radiochemical experiment, targeting solar neutrinos, achieving the first detections in 1968 that led to the so-called “Solar Neutrino Problem” (section 2.2).

In those years, other experimental evidence was putting on crisis the models for the weak interaction. One of these results was, for example, the “ $\tau - \theta$ puzzle”. It was experimentally seen that two particles, τ and θ , with the same mass, spin, and lifetime had different (weak) decay modes:

$$\begin{aligned} \tau &\rightarrow 2\pi, & l = 0, & P = P_\pi^2 = +1 \\ \theta &\rightarrow 3\pi, & l = 0, & P = P_\pi^3 = -1. \end{aligned} \quad (2)$$

To explain this, Yang and Lee in 1956 proposed that weak interactions could violate parity [8]. In the same article, a simple proposal for an experiment was also made:

Select a nucleus which has an intrinsic spin and which decays radioactively by emitting high-speed electrons. Orient a bunch of such nuclei so that their spins are in the same direction - say counterclockwise when viewed from above. Count the numbers of electrons emitted upward and downward.

They were awarded the Nobel prize one year later after parity violations were observed in the β decay of polarized ^{60}Co by Wu et al [9]. To demonstrate that a process violates a symmetry, it is enough to show that a distribution that characterizes it depends on a parameter changing sign under this symmetry. In the experiment, the direction of emission of electrons emitted by the decay $^{60}\text{Co} \rightarrow ^{60}\text{Ni}^{\star} + e^{-} + \bar{\nu}_e$ was measured. The Co atoms were polarized through an external magnetic field to have a uniform direction of the spin of the nuclei. With this setup it was observed that electrons are emitted preferentially in the direction opposed to the spin of the Co nuclei, proving that parity is not conserved in β decays.

A striking consequence of the violations of parity of the weak interaction is that neutrino spin and momentum cannot be aligned randomly, but are in two very precise states: for neutrinos, the spin is always opposite to the momentum and this is referred to as “left-handed”, whereas the anti-neutrinos are always “right-handed”. This property is called “helicity”, defined as the projection of the spin of the particle onto the direction of momentum. The neutrino helicity was measured in 1958 in a fundamental experiment by Goldhaber, Grodzins, and Sunyar [10] using the decay chain by electron capture of Europium, concluding that (anti-)neutrinos must be (right-) left-handed.

These seminal experiments were fundamental for the development of the full theory for the weak interaction as they directly relate to the V-A (Vector-Axial) structure of the charged current W^{\pm} weak interaction vertex, illustrated on Figure 5. The theory also introduces neutral current interactions that are mediated by the Z boson, as shown in the same figure.

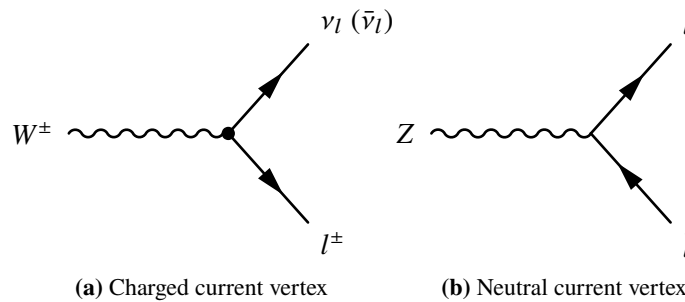


Figure 5: Illustration of the weak interaction vertices involving neutrinos.

Only the left-handed components of particles and right-handed components of anti-particles participate in charged current weak interactions [11]. For massless particles, and in the very high energy limit ($E \gg m$) for massive ones, the left-handed components are helicity eigenstates: -1 for left-handed particles, and $+1$ for right-handed antiparticles. In this regime, it is therefore possible to directly probe the chirality of weak interactions through the measurement of the helicity of neutrinos.

1.2.4 Different neutrino flavors

Another puzzling observation was that neutrinos produced along with an electron or positron always produced back an electron or positron through CC weak interactions while the expected decay $\mu^- \rightarrow e^- + \gamma$ mediated by the diagram shown in Figure 6 was not observed:

$$BR(\mu^- \rightarrow e^- + \gamma) < 10^{-11}. \quad (3)$$

This suggested that neutrinos produced in β decays ($n \rightarrow p + e^- + \bar{\nu}_e$) and in pion decay ($\pi^+ \rightarrow \mu^+ + \nu_\mu$) are distinct particles.

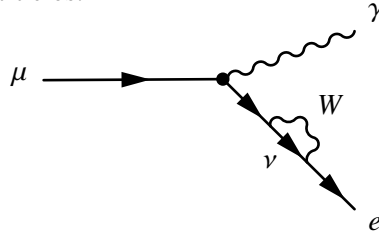


Figure 6: Diagram of $\mu^- \rightarrow e^- + \gamma$ interaction.

To experimentally observe this new “muon” neutrino, an intense source is needed. In the early 1960s, it was realized that particle colliders could be used to produce intense high-energy neutrino beams: the collision of high-energy protons with a target produces secondary particles, among which there are abundant pions. These in turn decay into muons and neutrinos. Finally, the beam is passed through a shield to stop the muons, extracting only the neutrinos. Moreover, in 1960, Lee and Young estimated that the neutrino-nucleon cross-section at high energies (\sim GeV) is directly proportional to the neutrino energy ($\sigma \propto G_F^2 E_\nu^{\text{lab}}$), and therefore smaller experiments (compared to previous reactor ones) could be used. This was the basis for the Brookhaven experiment of 1962 [12]: using a 15 GeV proton beam for the production of neutrinos and a spark chamber to distinguish between the tracks left from ν_e and ν_μ , they successfully observed and distinguished for the first time muon neutrinos. This discovery was awarded the Nobel Prize in 1988.

The observation in 1975 of a third generation of charged leptons, the τ , initiated the race for the detection of a third generation of neutrinos. The existence of this third generation of neutrinos was confirmed indirectly in 1989 [13] through the measurement of the invisible decay width of Z boson $Z \rightarrow \nu_l + \bar{\nu}_l$. Tau neutrinos were observed directly in 2000 with the DONUT experiment at Fermilab [14].

1.2.5 Neutrino interactions

The V-A structure of the weak interaction vertex implies that neutrinos couple through weak currents only with left-handed u and d quarks (right-handed \bar{u} and \bar{d} for anti-neutrinos). When computing the interaction amplitudes [3], this leads to sizeable different cross sections for neutrinos and anti-neutrinos (Figure 7). At energies above few GeV, neutrinos interact directly with the quarks in the atomic nuclei (called “partons”) through the so-called “deep inelastic scattering” and we have $\sigma(\nu N)/\sigma(\bar{\nu}N) \sim 2$ at GeV–TeV energies. This ratio is getting closer to 1 at very high energies.

As we will see in section 3.1, the discovery of this regime has been fundamental for the development of neutrino astronomy. The difference in the cross section between neutrinos and anti-neutrinos is also key for the measurement of the neutrino mass ordering with atmospheric neutrinos. A detailed review of neutrino interactions is available in [15].

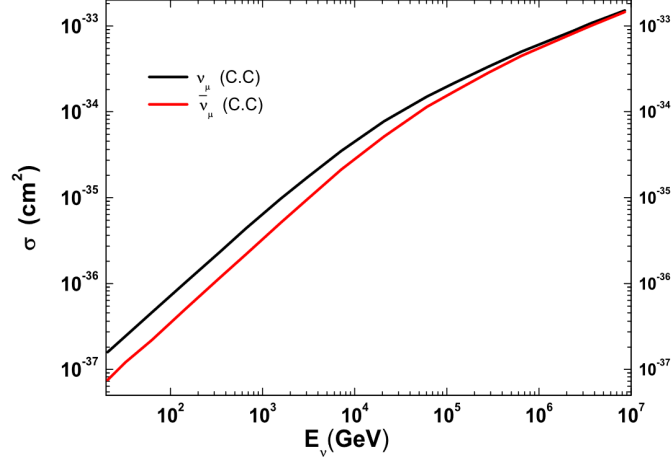


Figure 7: Cross sections of neutrinos and anti-neutrinos on quarks in the deep inelastic scattering regime [16].

2. Neutrino Astronomy

2.1 Scientific motivations

To understand the physical processes involved in astrophysical sources, it is essential to observe the sky across various energy ranges, as they may carry complementary information regarding their emission process. An excellent example of the success of the multi-wavelength astronomy across the electromagnetic spectrum is the study of the Andromeda galaxy, where every wavelength band probed different emission processes:

- *Optical Band:* blackbody/thermal emission from stars.
- *Ultraviolet Band:* blackbody/thermal emission from massive stars.
- *Infrared Band:* emission from dust in molecular clouds, i.e. dense gas concentrations hosting star formation sites; different dust composition radiate at different energies.
- *Sub-millimeter/Radio Band:* both thermal (bremsstrahlung: photon emission from an electron after being deflected by a charge) and non-thermal (synchrotron: photon emission from an electron in a magnetic field) emissions from gas in molecular clouds.
- *X-ray Band:* both thermal (blackbody and bremsstrahlung from gas in galaxy clusters and accretion onto compact objects) and non-thermal (synchrotron and inverse Compton: low-energy photon scattering on a charged particle, getting transferred part of its energy) emissions.
- *Gamma-ray Band:* non-thermal emission from inverse Compton scattering and from the interaction of high-energy protons with the interstellar gas (Equation 4). This is a promising band for multi-messenger observations as hadronic processes will also produce cosmic rays

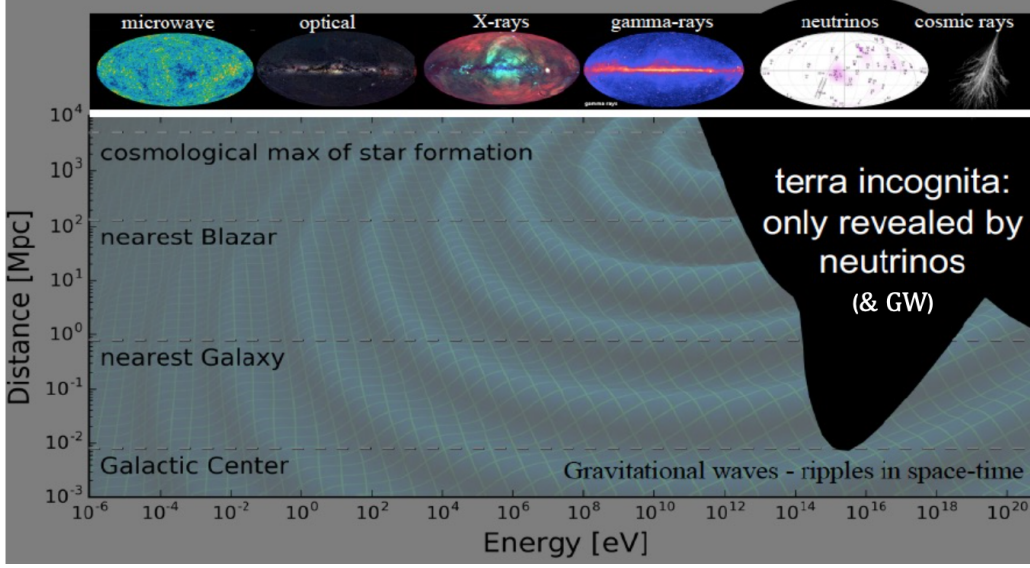


Figure 8: Distance horizon at which the universe becomes non-transparent to electromagnetic radiation as a function of photon energy [17].

and neutrinos in large quantities through the decay of charged mesons (e.g., pions):

$$p + p \rightarrow p + p + \pi^0 \quad ; \quad \pi^0 \rightarrow \gamma + \gamma \quad (4)$$

$$\rightarrow p + n + \pi^+ \quad ; \quad \pi^+ \rightarrow \mu^+ + \nu_\mu \quad ; \quad \mu^+ \rightarrow e^+ + \nu_e + \bar{\nu}_\mu \quad (5)$$

Multi-messenger astrophysics is a natural extension of multi-wavelength astronomy, where the different electromagnetic wavelengths are replaced by different messengers that probe various phenomena within astrophysical sources. Neutrinos have some particular properties that make them ideal candidates for multi-messenger searches:

- As they have no electric charge, neutrinos are not affected by magnetic fields and can travel in a straight line from the source to Earth.
- Thanks to their tiny interaction cross section, they can easily propagate through dense environments (both at the source where they are produced and on the way to the observer) without being absorbed.
- They are signatures of hadronic acceleration processes and therefore carry vital information on cosmic accelerators.

Neutrinos are thus the sole messenger (together with Gravitational Waves) to be able to probe the high energy sky over cosmological distances (Figure 8).

2.2 Historical aspects

2.2.1 First ideas

Already in 1960, Reines realized that [18]:

[Neutrinos] propagate essentially unchanged in direction and energy [...] and so carry information which may be unique in character. For example, cosmic neutrinos can reach us from other galaxies whereas the charged cosmic ray primaries reaching us may be largely constrained by the galactic magnetic field. [...] At present no acceptable theory of the origin and diffusion of cosmic rays exists so that the cosmic neutrino flux can not be usefully predicted. An observation of these neutrinos would provide new information as to what may be one of the principal carriers of energy in intergalactic space.

In the same year, Greisen, in a couple of papers, proposed the possibility of doing high-energy neutrino astronomy together with the first idea of a detector [19]:

We propose a large Cherenkov counter, about 15 m in diameter, located in a mine underground. [...] The mass of the sensitive detector could be about 3000 tons of inexpensive liquid. [...] For example, from the Crab nebula the neutrino counting rate would be one count every three years [...] the background can be made just as small. [...] Fancyful though this proposal seems, we suspect that within the next decade, cosmic ray neutrino detection will become one of the tools of both physics and astronomy.

Although it was assumed that neutrinos could be easily observed at high energies, the first astrophysical neutrino detections, which occurred a few years later, were of neutrinos from the Sun and from one supernova.

From thermonuclear fusion models, it was known that neutrinos coming from the Sun should have been observed, with an estimated flux

$$\Phi_\nu = 2 \times \frac{L_{Sun}}{Q} \times \frac{1}{4\pi R^2} = 2 \times \frac{3.8 \times 10^{26} \text{ W}}{27 \text{ MeV}} \times \frac{1}{4\pi(5 \times 10^{11} \text{ m})^2} \approx 6.3 \times 10^{10} \text{ cm}^{-2} \text{ s}^{-1} \quad (6)$$

and a complex spectrum extending up to tens of MeV (Figure 9). Given the huge expected flux, a lot of study was dedicated to the detection of solar neutrinos and two experimental approaches were proposed: radiochemical experiments and real-time detection experiments.

2.2.2 Detection of solar neutrinos

Radiochemical experiments, first proposed by Pontecorvo in 1946 (see section 1.2), are based on the counting of daughter nuclei produced after neutrino capture on neutrons of the parent atoms ($\nu_e + {}^Z_A X \rightarrow {}^{Z+1}_A Y + e^-$). For solar neutrinos, this results in a capture rate of $\sim 10^{-36} \text{ atom}^{-1} \text{ s}^{-1} \equiv 1 \text{ SNU}$ (Solar Neutrino Units). Still, the low energy threshold together with an excellent background rejection and the possibility of taking very long exposures have made this technique very efficient.

Indeed, the first detection of solar neutrinos took place with the Homestake experiment [21], located in the Homestake Gold Mine in South Dakota, USA. The project, led by Raymond Davis Jr., aimed at capturing neutrinos emitted by the Sun through their interaction with a large tank of cleaning fluid ($\sim 615 \text{ t}$), primarily composed of perchloroethylene (C_2Cl_4). The experiment began its operation in the late 1960s, with data collection starting in the early 1970s. The initial results indicated that the number of detected solar neutrinos was notably lower than what was predicted by solar models: the averaged count rate resulted being $(2.56 \pm 0.20) \text{ SNU}$, 1/3 of the flux prediction

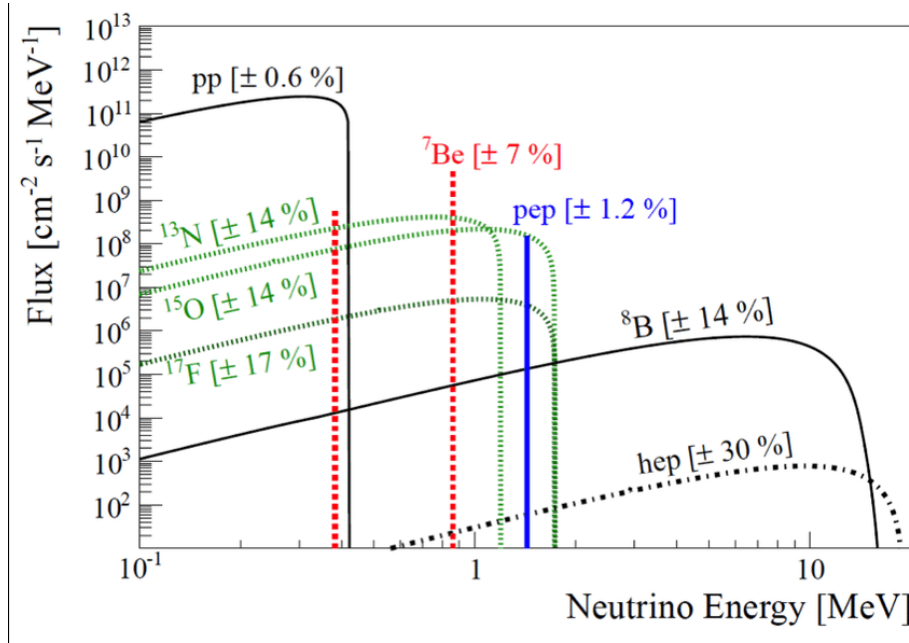


Figure 9: Spectrum of solar neutrinos with contributions from different processes [20].

based on the Standard Solar Model ((7.6 ± 1.2) SNU). This discrepancy between the predicted and observed neutrino flux became known as the “Solar Neutrino Problem”.

Real-time neutrino detection experiments, like Kamiokande (1987–1996) and Super-Kamiokande (1996–today), employ a large volume of transparent material, such as pure water (50,000 t for Super-Kamiokande), equipped with light-sensitive detectors (photomultiplier tubes) in order to identify neutrino interactions in real-time. When neutrinos interact with the material, they produce Cherenkov radiation, which is captured by the photo-detectors.

With this detection method, in 1998, the Super-Kamiokande collaboration managed to obtain the first neutrino image of the Sun between 5 and 20 MeV, thanks to the high directionality performance that allowed to unequivocally identify the origin of the neutrinos. This measurement also confirmed the ν_e deficit already observed in radiochemical experiments [22], which could only be explained with oscillations, as described in the next paragraphs.

To complete the picture of 20th-century detections of astrophysical neutrino sources, in 1987, 24 neutrinos of about 10 MeV were detected by Kamiokande, IMB and Baksan experiments in a few seconds duration burst about 3 hours before the electromagnetic emission of the supernova SN1987A. The neutrinos were emitted along the core collapse of a massive star in the Large Magellanic Cloud (a dwarf galaxy, satellite of the Milky Way) at the end of its life.

These first detections of solar and supernova neutrinos were awarded the Nobel Prize in Physics in 2002 [23].

2.3 Oscillation detour

To solve the solar neutrino problem and interpret it as neutrino oscillations, an ideal experiment would need huge event statistics to detect different neutrino flavors from a common, well-known source. This is difficult, since the experimental configuration, including the distance to the source

(L) and the energy range (E), determines the sensitivity to oscillation parameters such as the mixing angle (θ) and the mass squared difference (Δm^2). Ideal experiments would have point-like sources, mono-energetic neutrinos of a single flavor, and known intensities.

However, in reality, there are uncertainties in efficiency, flavor identification, energy calibration, and background estimation. For this reason, different experiments have been built, studying the different sources known at the time: solar, atmospheric, reactor, and beam neutrinos. The decisive results that solved the solar neutrino problem were reached by the Sudbury Neutrino Observatory (SNO, able to detect all neutrino flavors) studying solar neutrinos [24] and by Super-Kamiokande a few years earlier studying atmospheric neutrinos [25].

Atmospheric neutrinos are produced in the interactions of cosmic rays with the atmosphere, mainly through the decay of pions in muons and electrons $\pi^+ \rightarrow \mu^+ + \nu_\mu \rightarrow e^+ + \nu_e + \bar{\nu}_\mu + \nu_\mu$. These decays lead to a flavor ratio $\nu_\mu : \nu_e : \nu_\tau = 2 : 1 : 0$ in a wide energy range (1-20 GeV), with no tau neutrinos produced. Neutrino flavor mixing is governed by the PMNS matrix illustrated in Figure 1a. If only two flavors are considered (in this case μ and τ), the probability of a neutrino not changing its flavor is given by

$$\begin{aligned} P_{\nu_\mu \rightarrow \nu_\mu} &= 1 - P_{\nu_\mu \rightarrow \nu_\tau} \\ &= 1 - \sin^2 2\Theta_{23} \sin^2 \left[1.27 \frac{\Delta m_{23}^2 L}{E} \right], \end{aligned} \quad (7)$$

which is sensitive to the ratio L/E , as illustrated in Figure 10. This behavior was confirmed in 1998 by Super-Kamiokande when the zenith distribution of atmospheric electron and muon neutrinos were measured (Figure 11). The angular distribution of ν_e -like interactions came out consistent with the absence of oscillations, while a deficit of upgoing ν_μ -like events i.e., passing through the Earth, with respect to downgoing ones (originating from the atmosphere above the detector), was found to be in agreement with the theoretical prediction for $\nu_\mu \leftrightarrow \nu_\tau$ oscillations (ν_μ disappearance) [26].

A few years later, the definitive confirmation of neutrino oscillations arrived from the observations of solar neutrinos by SNO. Located underground in Ontario (Canada), SNO used a 10000 photomultiplier tube (PMT) detector filled with heavy water (D_2O) to study solar neutrinos. Such a configuration allowed measuring both the all-flavor flux using neutral current interactions ($\nu_x + d \rightarrow p + n + \nu_x$, detected thanks to the neutron capture on a deuteron), and the electron neutrino flux alone with charged current interactions ($\nu_e + d \rightarrow p + p + e^-$). An additional channel related to elastic scatterings ($\nu_x + e^- \rightarrow \nu_x + e^-$) provides a cross-check of these measurements.

SNO measured a flux of electron neutrinos in agreement with previous findings, while the total flux of active neutrinos ($\nu_e + \nu_\mu + \nu_\tau$) from 8B decay in the Sun corresponded to

$$\Phi_{\nu_x}({}^8B) = (5.25 \pm 0.16_{\text{stat}} \pm 0.13_{\text{sys}}) \times 10^6 \text{ cm}^{-2} \text{ s}^{-1}. \quad (8)$$

This value is in perfect agreement with the predictions from the Standard Solar Model [28, 29] and therefore is a confirmation that neutrinos do undergo oscillations on their propagation from the Sun core to Earth.

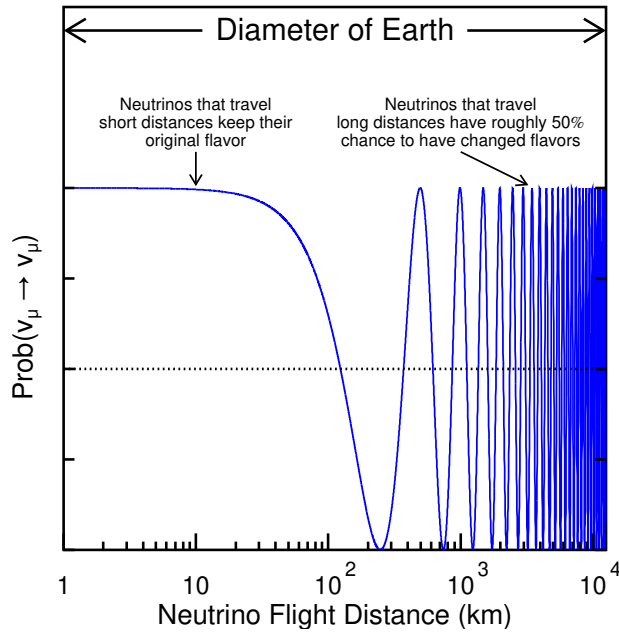


Figure 10: Probability of a muon neutrino not changing its flavor vs. the ratio L/E , in the two-flavour approximation.

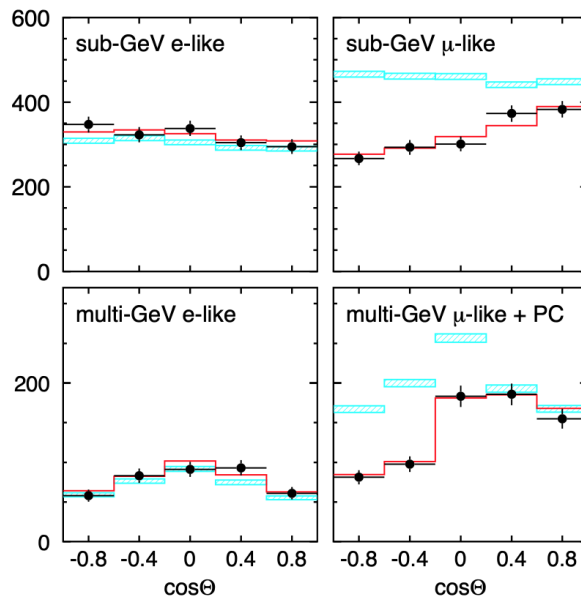


Figure 11: Zenith angle distributions of e -like and μ -like events in Super-Kamiokande with momenta above and below 1.33 GeV [27]. The blue boxes show the expectation assuming no oscillations, while the plain red lines show the results of the best fit with oscillations.

2.4 Cosmic neutrino sources

As we have discussed in the previous section, neutrinos from the Sun and supernovae had already been observed by the 2000s. These discoveries pushed forward the development of new instruments to detect cosmic neutrinos with energies above the GeV scale.

Similarly to the discussion on photons in [section 2.1](#), neutrinos with different energy bands are emitted in astrophysical sources, through different mechanisms. Low-energy MeV neutrinos coming from the Sun and supernovae were already discussed in the previous paragraphs.

At higher energies, astrophysical neutrinos are mostly produced by the processes responsible for the acceleration of cosmic rays (highly-energetic atomic nuclei) by both galactic and extra-galactic sources ([Equation 5](#)) and, hypothetically, by decays/interactions of dark/exotic matter. High-energy neutrinos are therefore tracers of radiative processes at the highest energies, bringing information otherwise inaccessible via other cosmic messengers about the production and acceleration of ultra-high-energy cosmic rays (UHECR). Cosmic rays, being charged particles, do not travel in a straight line, being deflected by magnetic fields, and it is therefore almost impossible to trace the sources of the individual signals.

The acceleration mechanisms must satisfy two criteria: they must provide enough energy to reach the largest observed energies and the accelerated population should have an injection energy spectrum that fits the observed UHECR spectrum after propagation. Generic acceleration models were first proposed by Fermi [[30](#)]. They rely on the presence of a magnetic field in a sufficiently extended region. One may compute the maximum energy E_{\max} a cosmic ray of charge q could be accelerated to, in a spatial region of dimension L with a magnetic field B :

$$\begin{aligned} E_{\max} &= qLB \\ &\simeq q \cdot \left(\frac{B}{1 \mu\text{G}} \right) \cdot \left(\frac{L}{1 \text{kpc}} \right) \quad [\text{EeV}]. \end{aligned} \quad (9)$$

Above this threshold, the particle is able to escape the region. This defines the Hillas criterion for cosmic rays: every possible galactic and extra-galactic source must be above the line in [Figure 12](#), to be considered valid cosmic ray accelerators.

2.4.1 Extra-galactic sources

Considering the classification of interesting sources obtained with [Figure 12](#), we can list a few promising candidates of extra-galactic sources of astrophysical neutrinos:

- **Active Galactic Nuclei (AGN)** [[31](#), [32](#)]: a small region located at the core of certain galaxies that exhibits a significantly higher luminosity than what can be attributed solely to the resident stellar population. This exceptionally radiant central region emits so much radiation that it can overshadow the entire galaxy. AGNs are prolific sources of electromagnetic radiation spanning the entire spectrum, from radio waves to gamma rays. This radiation emanates from the accretion of matter onto a central supermassive black hole. There are many different types of AGN, depending on the mass of the central black hole, the presence of a radio emission, the presence of a jet, and its luminosity. The most powerful AGNs are known as *quasars*, which give rise to extremely luminous galactic centers. A *blazar* is an AGN with a relativistic jet of ionized matter pointed toward the Earth.

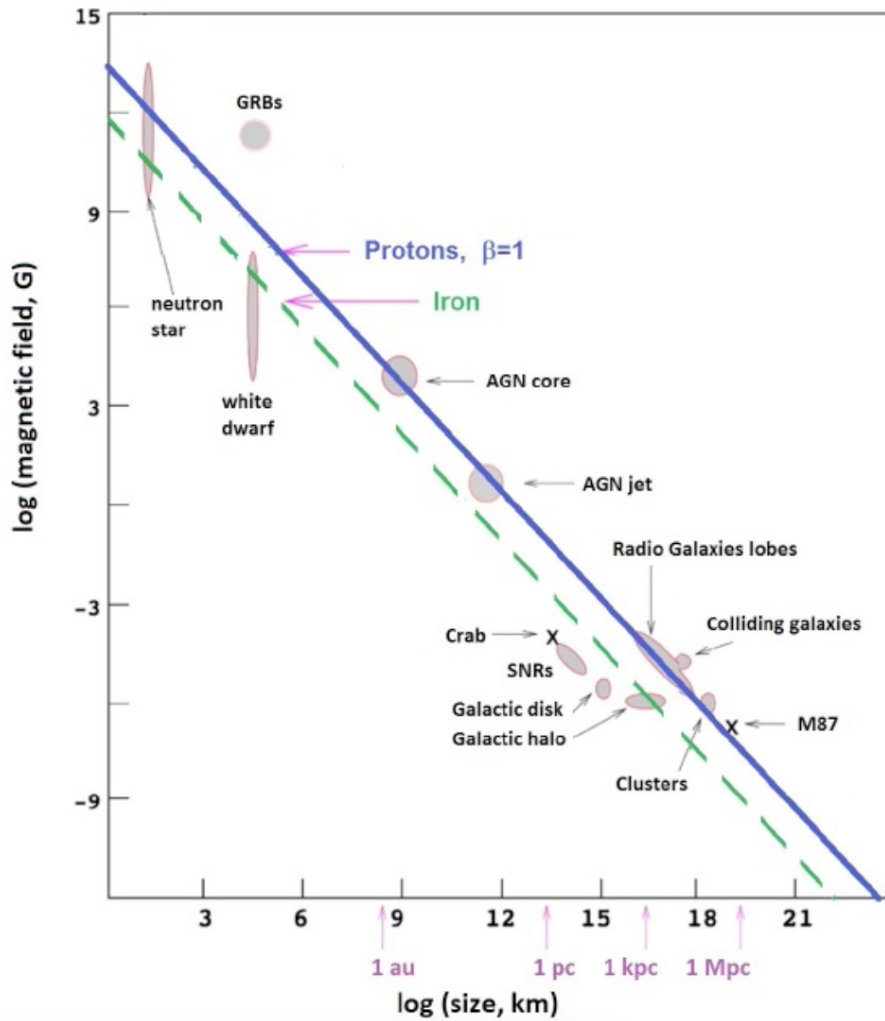


Figure 12: Hillas plot from [16]. The sources above the solid (dashed) have the characteristics (in terms of size and magnetic field intensity) to accelerate protons (iron) up to 10^{20} eV.

- **Gamma Ray Burst (GRB)** [33, 34]: flashes of gamma-ray photons lasting between a few milliseconds and several hours from extremely energetic cosmic explosions. With luminosities up to about $10^{18} L_{Sun}$ GRBs are among the most luminous (transient) sources of radiation in the universe. According to their duration, GRBs fall into either of two groups: *Long GRBs* (LGRB) typically lasting tens of seconds, associated with type Ib/c supernovae (they are assumed to originate from collapsars, massive evolved stars, core-collapsing into a black hole) and *Short GRBs* (SGRB) usually lasting less than one second and assumed to be caused by mergers of compact objects in binary systems, like two neutron stars or one neutron star and one stellar black hole.
- **Starburst Galaxies** [35, 36]: galaxies undergoing an exceptionally high rate of star formation compared to the average rate in most other galaxies. In particular, supernova explosions may produce a large flux of cosmic rays that will subsequently interact with interstellar nucleons,

producing high-energy pions that further decay to neutrinos.

Beyond these main categories, other astrophysical phenomena may emit neutrinos, such as tidal disruption events (a star pulled apart by the gravitational force exerted by a stellar black hole) [37], fast radio bursts [38], or galactic halos [39].

2.4.2 Galactic sources

Our Galaxy, the Milky Way, hosts about 100 billion of stars and a supermassive black hole in its center. We expect about one supernova per century to occur in the Milky Way. This astrophysical event would provide a huge number of MeV neutrinos to detectors scattered around the world, providing a unique opportunity to study the underlying mechanisms and to probe the neutrino properties.

The Galaxy is also a very promising source of higher-energy neutrinos. Indeed, through gamma-ray observations [40], we have evidence that it hosts PeVatrons, sources that accelerate cosmic rays up to PeV energies. The exact nature of these sources is not yet precisely known, though supernova remnants (large structures resulting from the explosion of a star into a supernova) are promising candidates [41]. The Galactic Centre itself, as it hosts a supermassive black hole of about $4 \times 10^6 M_{\odot}$ surrounded by dense environments, is also a strong candidate to infer neutrino emission.

Other galactic sources include:

- **Microquasars** [42, 43]: X-ray binaries with a compact object (neutron star or black hole) accreting matter and re-emitting it in relativistic jets (intense radio and infrared) flares.
- **Soft Gamma Repeaters** [44, 45]: X-ray pulsars with a soft gamma-ray bursting activity. The magnetar model suggests that these are highly-magnetized neutron stars whose outbursts are caused by global star-quakes.

3. Neutrino Telescopes

3.1 Detection principle

The story of astrophysical neutrinos from their production to their identification can be summarised in a few steps:

1. Emission from a multi-messenger source, potentially in coincidence with other messengers (photons, gravitational waves, ...).
2. Neutrinos will travel toward the Earth, eventually traversing it and arriving at the detector.
3. Neutrinos will interact with the medium, producing charged particles. If the interaction is through charged current, a lepton will be produced, while neutral current interactions are associated with the generation of a hadronic shower.
4. If energetic enough, the charged particles will induce Cherenkov light in the medium.
5. This radiation is collected by the Optical Modules (OM) of the detector and converted to an electric signal that can be saved for analysis.

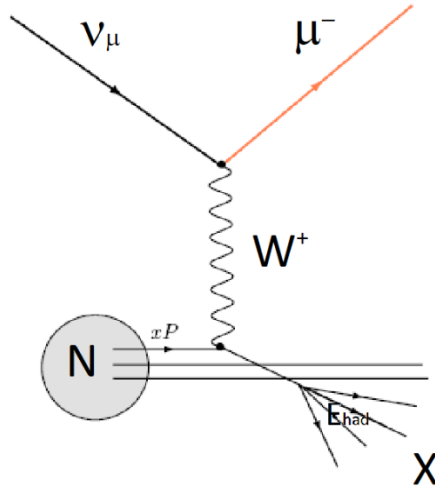


Figure 13: Feynman diagram of neutrino-nucleus Deep Inelastic Scattering.

6. By reconstructing the topology of the Cherenkov emission, it is then possible to estimate the properties of the original neutrino.

At energies above a few GeV, neutrino interactions occur mostly via the so-called “deep inelastic scattering (DIS)” (Figure 13). High energy neutrinos interact with partons of the nucleons, via either charged current (CC) weak interactions ($\nu_l + N \rightarrow l + X$ with $l = e, \mu, \tau$) or neutral current (NC) ($\nu_l + N \rightarrow \nu_l + X$).

The detection then relies on the Cherenkov effect discovered in 1934 by Pavel Cherenkov [46]. This radiation consists of the coherent emission of light produced by relativistic charged particles moving in a medium faster than the speed of light in this medium. The charged particles polarize the molecules of the medium, which then turn back rapidly to their ground state emitting radiation in a cone of angle θ_C with

$$\cos \theta_C = \frac{1}{\beta n}, \quad (10)$$

where β is the speed of the particle and n is the refraction index of the medium. The amplitude of this angle is important for reconstructing the direction of arrival of the incoming neutrino. This immediate Cherenkov light detection enables prompt event analysis, allowing the estimation of the incoming direction of the neutrino.

To emit Cherenkov light, a charged particle must move faster than the speed of light in the medium, which depends on its refraction index n , $\beta > \frac{1}{n}$. This places a strong constraint on the energy of the incoming particles for them to be detected: $E > E_{\text{threshold}} = \gamma m c^2 = \frac{1}{\sqrt{1 - (\frac{1}{n})^2}} m c^2$. In water, this corresponds to an energy threshold of 0.775 MeV (160.3 MeV) for electrons (muons).

This scheme for the detection of astrophysical neutrinos was already proposed in 1961 by Markov [47]. In his paper, Markov proposes the use of muons as a great candidate for the indirect detection of ν_μ for several important reasons.

Muons can travel long distances: in water, a 1 TeV (1 PeV) muon can travel for up to 3 km (10 km). A charged current interaction of a muon neutrino will produce a muon. This process

does not need to happen inside the volume of the detector itself, but could also happen outside of it, greatly increasing the effective volume for the detection ($V_{\text{eff}} \gg V_{\text{detector}}$), compensating for the very small probability of interaction.

Moreover, both the interaction cross section for the ν_μ , as well as the transferred energy to the muon E_μ itself increase with the particle energy, causing the effective volume to also grow with the energy of the incident neutrino E_ν . This also means that the angle between the incident neutrino and the outgoing muon decreases with E_ν since, the higher this value is, the greater the boost given to the muon, effectively making the particles collinear and increasing the sensitivity to the arrival direction.

For these reasons, Markov advanced the first proposal for a modern type of neutrino detector: a 3D array of photomultiplier tubes (PMT) “deep in a cave or sea”, to get the biggest effective volumes possible.

Modern detectors use variations of this initial design, putting big arrays of PMTs under water or in polar ice. From the time, position, and amplitude (i.e., the number of photons detected) of PMT pulses it is then possible to reconstruct the muon energy and trajectory with great accuracy (e.g. angle sensitivity $\sim 0.5^\circ$ in water).

Different channels of interaction (see also section 2.3) lead to different topologies of the signal in the PMT array (different shapes of the Cherenkov emission and of the particle shower):

- **Track-like events:** golden channel described by Markov for ν_μ charged current interactions. As the muon is collinear with the neutrino and has a relatively long path length (see Figure 14), this channel leads to very good angular resolutions ($\sim 0.1 - 0.5^\circ$). The energy resolution is quite poor because the interaction may have happened outside the detector volume and it is therefore difficult to estimate the initial muon energy.
- **Shower-like events** (also called cascade events): ν_e charged current interactions or neutral current interactions of any flavor producing a cascade over a few meters. Focusing on interactions taking place inside the detector volume, it is thus possible to reconstruct precisely the neutrino energy by accounting for the total light deposit. As the event topology is quite spherical, the angular resolution is worse than for track-like events (from 1° to $> 10^\circ$).
- **Double-Bang events:** these are double cascade events typical of ν_τ charge current interactions. The first cascade is produced by the neutrino interaction ($\nu_\tau + N \rightarrow \tau^- + X$) while the second cascade occurs when the τ subsequently decays inside the detector volume. As can be seen in Figure 14, the τ has a non-negligible path length at very high energies, which allows separating the two cascades and provides a lever arm for determining the original neutrino direction.

The interaction length of a particle is $\lambda = 1/(n\sigma)$ where n is the number density of nucleons and σ is the interaction cross section. The surviving fraction of particles after propagation on a distance x is thus $f(x) = e^{-x/\lambda}$. A 1 TeV gamma ray has an interaction length (in water) of $\lambda = 42$ cm, while a 1 TeV neutrino has $\lambda \sim 2 \times 10^9$ m. The increase of the neutrino cross section with energy is such that the Earth absorption becomes not negligible for energies above 100 TeV, as illustrated on Figure 15. Thus, Earth is opaque to very-high-energy neutrinos and horizontal tracks become the “golden channel”, at the cost of a more limited effective volume.

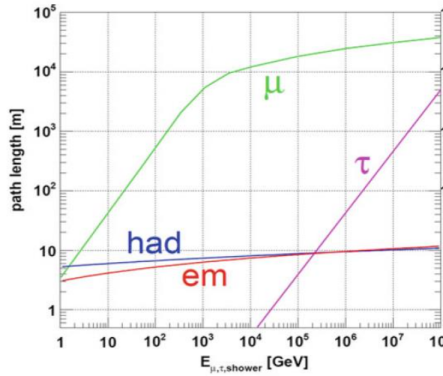


Figure 14: Path length of particles produced by different neutrino flavors and interactions in water versus their respective energy [48].

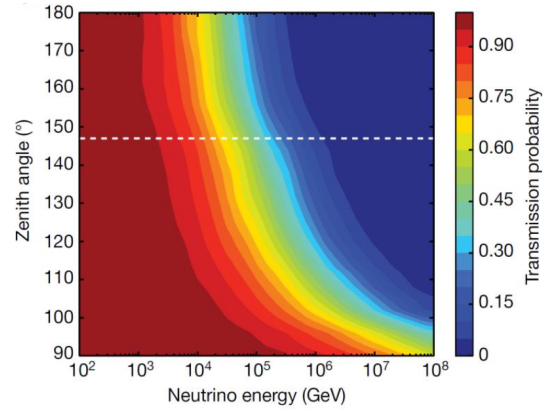


Figure 15: Transmission probability of neutrinos through Earth as a function of zenith angle and energy.

In modern detectors, PMTs are inserted into optical modules (OMs) arranged in single lines immersed in water or ice to form a 3D array of detectors. Focusing on neutrinos with energies above a few GeV, it is possible to space the modules by several meters without losing any signal, as even GeV electrons and muons would produce a track longer than 10 m in the medium.

Two main sources are contributing to the optical background in seawater: the decay of radioactive elements present in water, and the bioluminescence linked to microorganisms. The dominant radioactive isotope is ^{40}K and the electron produced during its decay is above the threshold for Cherenkov light production. On the contrary, the deep polar ice is almost free from radioactive elements, having therefore almost no optical background.

Another important factor is the light propagation in the medium, namely the absorption and the scattering of photons. These affect the reconstruction capabilities of the telescope. Both water and ice are transparent only for wavelengths $300 \text{ nm} < \lambda < 600 \text{ nm}$, i.e. in the blue-UV region. In this range, the absorption length is $\sim 100 \text{ m}$ for deep polar ice, while it is $\leq 70 \text{ m}$ for seawater (see Figure 16). It is therefore possible to cover a larger effective volume with the same number of detection units in ice than in seawater.

Scattering changes the direction of the Cherenkov photons, and consequently delays their arrival time on the PMTs degrading the measurement of the direction of the incoming neutrino. The effective scattering length for ice is smaller than water and this causes a large degradation of the angular resolution of detected events in ice.

Another important property of the medium is the homogeneity: as can be seen in Figure 17 the values of scattering length and absorption can vary widely in depth and wavelength. In particular, air bubbles present in the uppermost section of polar ice greatly increase the scattering. The event reconstruction is therefore more difficult and it requires detailed Monte Carlo simulations to account for these effects. In contrast, seawater is a particularly homogeneous medium.

Figure 18 shows one typical optical module configuration used in a modern neutrino detector. The PMT quantum efficiency, which quantifies the detection efficiency of incoming photons, is maximal within the wavelength range $300 - 600 \text{ nm}$, matching well the region of the Cherenkov

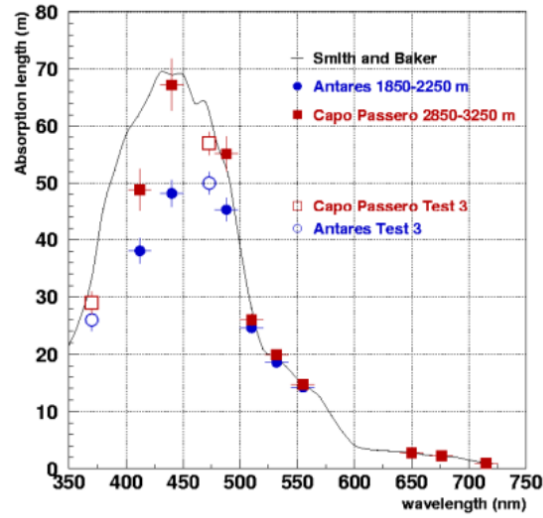


Figure 16: Absorption length as a function of wavelength in seawater [16].

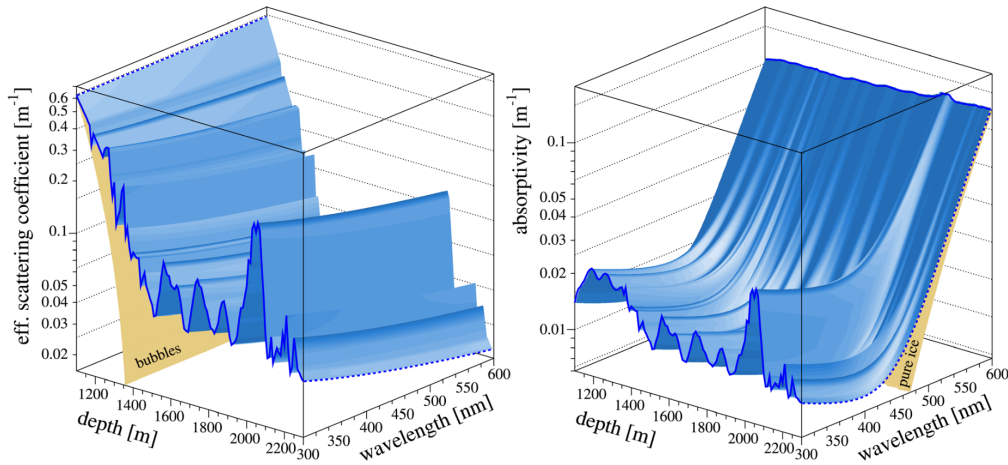


Figure 17: Maps of optical scattering and absorption for deep South Pole ice, as a function of the depth and wavelength [49].

radiation and in which ice and water are transparent to light.

To reconstruct the trajectory of a charged particle crossing the detector, the position and time of all detected hits in the PMTs are used. Considering that the Cherenkov radiation is emitted as a cone, the light deposit in the 2D plane of detection time versus z -position should follow hyperbolas as illustrated on Figure 19.

Atmospheric muons and neutrinos represent an important background for neutrino telescopes. Both downgoing and upgoing searches are affected by atmospheric neutrinos as these are expected to be coming from any direction. Atmospheric muons produced in cosmic-ray showers are partially absorbed before reaching the detector. For upgoing tracks, the Earth itself is acting as a shield so that no atmospheric muons survive. For downgoing tracks, despite the detectors being located deep in the sea/ice, the rate of atmospheric muons dominates by many orders of magnitude the rates of

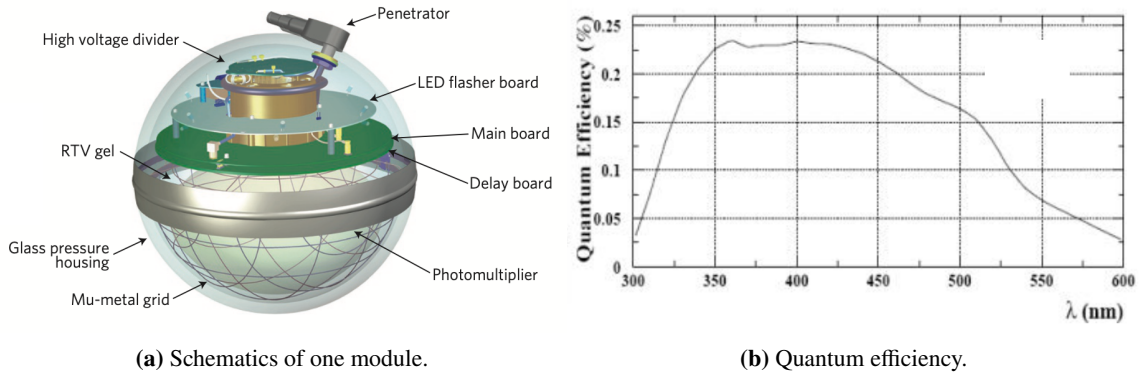


Figure 18: Digital Optical Module of the IceCube experiment [50].

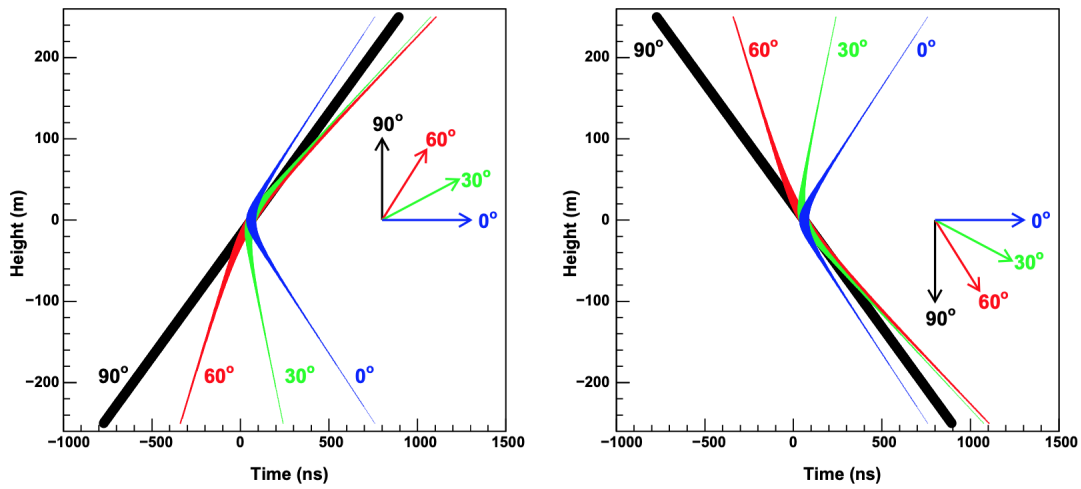


Figure 19: The pattern of Cherenkov light produced by a muon track on a single detector line (left panel: upgoing, right panel: downgoing). The point ($z = 0, t = 0$) is the point of closest approach between the track and the line. The colors correspond to different track angles and the line thickness indicates the brightness of the light signal. Figure from [51].

muons induced by neutrinos, as illustrated on [Figure 20](#).

Even though atmospheric and astrophysical neutrinos cannot be distinguished on an event-by-event basis, they follow different spectra, as shown on [Figure 21](#). The energy spectrum of atmospheric neutrinos (produced as secondaries in cosmic ray air showers) is steeper (typically $\propto E^{-3.7}$) than the one expected from cosmic neutrinos ($\propto E^{-2}$, following the cosmic ray spectrum as predicted by the Fermi acceleration mechanisms). This means that one may look for astrophysical neutrinos by selecting the events with the highest energies. Moreover, cosmic rays (subsequently producing atmospheric neutrinos) are expected to be evenly distributed across the sky and the presence of anisotropies (clusters of events) may indicate the presence of an astrophysical source.

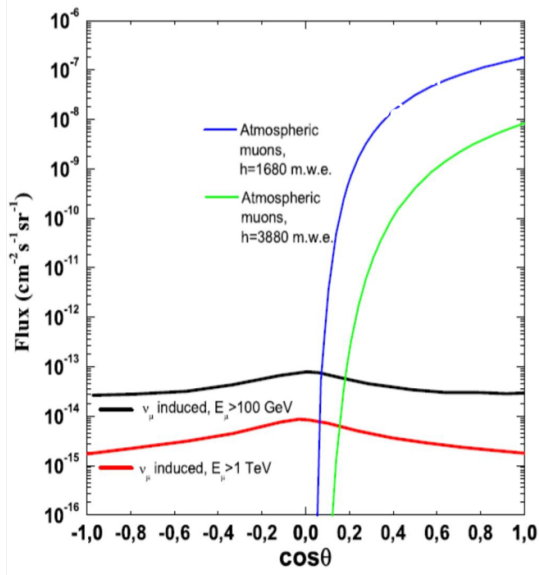


Figure 20: Atmospheric muon and ν_μ -induced muon fluxes as a function of the cosine of the zenith angle [52]. Atmospheric muons are shown for two different depths in seawater. For neutrinos, the fluxes above two different thresholds are reported.

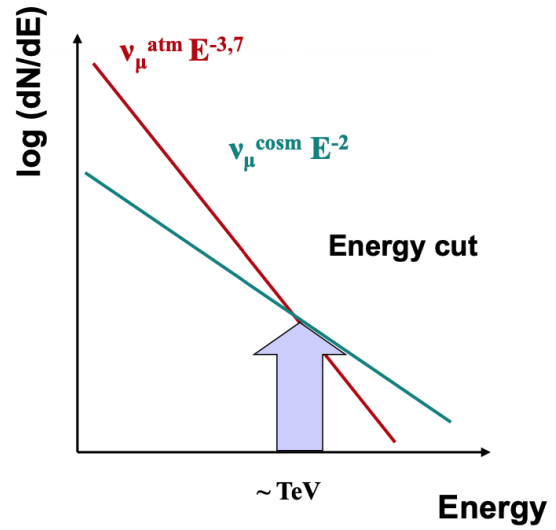


Figure 21: Spectra of atmospheric and astrophysical neutrinos. As they originate from different physical processes, the spectra are different and they intersect at the TeV scale.

3.2 Past and current telescopes

Currently, there are three main observatories for high-energy astrophysical neutrinos in the world: IceCube at the South Pole, KM3NeT in the Mediterranean Sea, and Baikal/GVD in the lake of the same name (Figure 22). However, there have been several smaller-scale projects going back to the 1980s.

The first project for a neutrino telescope using natural environments as a medium for the detection was the Deep Underwater Muon and Neutrino Detection experiment (DUMAND-II) in the Pacific Ocean [53]. DUMAND-II consisted of 9 strings and 216 OMs, aimed to be deployed at a depth of 4.8 km, 30 km from the coast of Hawaii. The first prototypes were tested during 14 cruises between 1982 and 1987, lowering the strings from the boat instead of anchoring them to the seafloor as it is done nowadays. However, in 1993, the first actual deployment of a string to the sea bed was a failure and the DUMAND-II project was terminated in 1995. This failure motivated the idea to use ice instead of seawater; the first such prototype was AMANDA [54], which was completed in 2000.

Thanks to the experience gained with AMANDA, another neutrino telescope in the ice was envisioned, IceCube [55], which is still the largest detector in the world. Completed in December 2010, IceCube consists of 86 strings, each equipped with 60 optical modules for a total of 5160 PMTs distributed to cover approximately one cubic kilometer. The PMTs are located at depths ranging from 1450 m to 2450 m, providing a natural shield from atmospheric muons. This impressive apparatus led in 2013 to the discovery of a diffuse flux of extraterrestrial neutrinos [56–59]. We will discuss these findings in section 4.1.

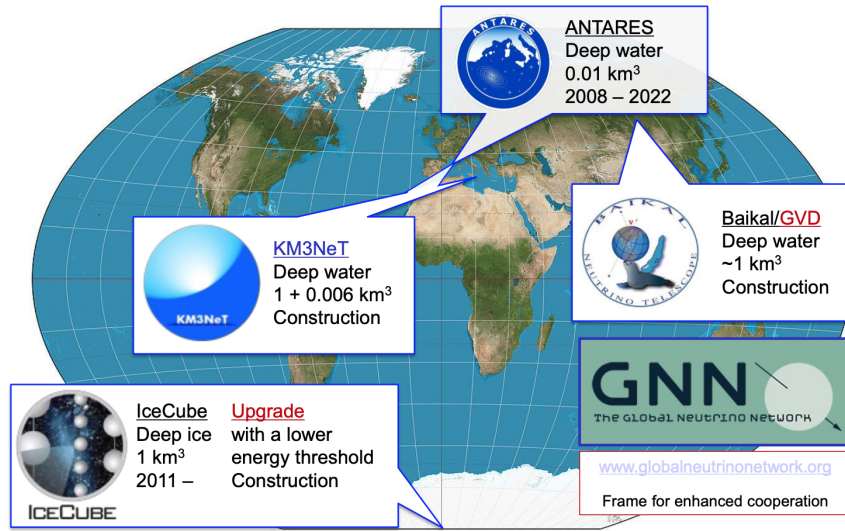


Figure 22: Global Neutrino Network as of September 2022.

The notable differences in terms of light propagation between ice and seawater described in section 3.1 pushed for the development of a new neutrino telescope that could complement IceCube observations. The choice fell on building a detector in the Mediterranean Sea for different reasons. First of all, a detector in the northern hemisphere would see neutrinos from the Galactic Center as upgoing, thus not contaminated by atmospheric muons, and therefore complementing the sky observable by IceCube. Seawater has a long and homogeneous scattering length that, as we have seen, yields very good pointing accuracy. Finally, the site is logistically attractive as it allows to put the detector in a very deep site (up to ~ 5000 m) while remaining fairly close to shore (easing deployments and data transfer).

The first successful instrument of this kind is the ANTARES detector [60], composed of 12 lines for a total of 885 PMTs and located off the coast of Toulon (France). It was completed in May 2008 and was decommissioned in 2022. Its successor, KM3NeT, is currently under construction [61]. It will be distributed over two locations in the Mediterranean Sea: KM3NeT/ORCA¹ (off Toulon, France), and KM3NeT/ARCA² (off Portopalo di Capo Passero, Sicily, Italy). The first lines have already been deployed, with some preliminary results being already produced [62].

The absolute pointing capabilities of such seawater-based experiments have been tested by looking at the Moon and Sun shadows. As they block the incoming flux of cosmic rays and therefore, their direction is associated with a reduced rate of atmospheric muons. For instance, ANTARES measurements [63, 64] conclude on an angular resolution of $(0.59 \pm 0.10)^\circ$, consistent with the simulations.

A drawback of putting the detector in seawater is the presence of a much higher optical activity compared to ice. Solving this requires causality filters but it may also be used for calibration purposes. Figure 23 shows the typical behavior of an ANTARES optical module. On average, each

¹Oscillation Research with Cosmics in the Abyss

²Astroparticle Research with Cosmics in the Abyss

OM has a baseline signal of ~ 60 kHz, determined by the decay of ^{40}K and by bioluminescence, plus some bursts of activity related to photo-emitter animals. This is taken into consideration in data analyses.

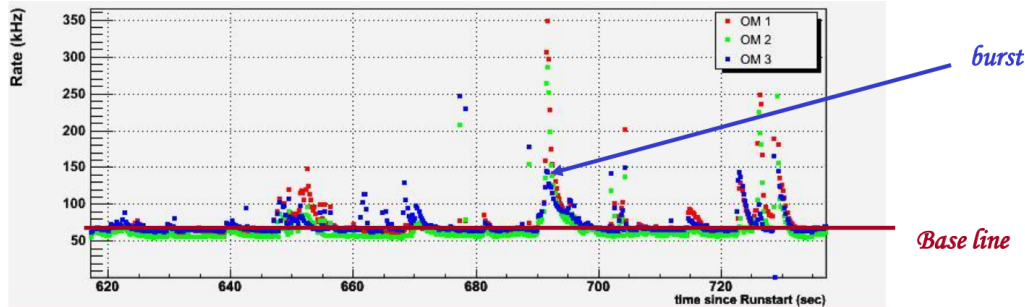


Figure 23: Typical behavior of ANTARES optical modules in the absence of a signal. In addition to a constant noise from the decay of ^{40}K (red baseline) the background is characterized by signal bursts given by the bioluminescence of some species of marine animals.

The noise due to bioluminescence and other animals is an interesting signal for other scientists. Both ANTARES and KM3NeT/ORCA are equipped with additional dedicated instrumentation lines focusing on these other topics in sea science, notably for the measurement of acoustic noises, mammal passages, and seismic activity. Therefore, the facility provides useful data for oceanographers, geophysicists, and biologists that already led to some studies [65–67].

4. Selected Results

4.1 Diffuse Flux

In 2013, IceCube announced the detection of two interesting cascade events. The analysis targeted EeV neutrinos, neutrinos produced by the interaction of cosmic ray protons with photons from the Cosmic Microwave Background (so-called GZK neutrinos [68, 69] or cosmogenic neutrinos). The two anomalous events were associated with a significance of 2.8σ [56].

The two cascades had an energy of about 1 PeV, very close to the energy threshold of the analysis. A further selection of “high-energy starting events” (“HESE” events) consisting of neutrino interactions starting in the detector with escaping muons, was developed to explore more in detail this energy regime. The PMT hits in the external layers of the detector were used as a veto against atmospheric muons, ensuring a high selection purity.

Using 2 years of IceCube data, 28 such events were identified, while only 11 events were expected from atmospheric muon and neutrino backgrounds, corresponding to a 4.1σ evidence for the existence of high-energy astrophysical neutrinos [57]. Subsequent analyses with larger data samples have confirmed this excess, with a significance $> 5\sigma$ [58, 59].

The distribution of HESE events for 6 years of data can be seen in Figure 24. It shows a clear excess at high energies which is not compatible with atmospheric backgrounds. The excess was fitted with a power-law $dN/dE = \Phi_0 E^{-\gamma_{\text{Astro}}}$ with a spectral index $\gamma_{\text{Astro}} \approx 2.92$. The most updated constraints on the spectral index and the related flux normalization are displayed in Figure 25, including constraints from complementary IceCube analyses (using different selections and samples).

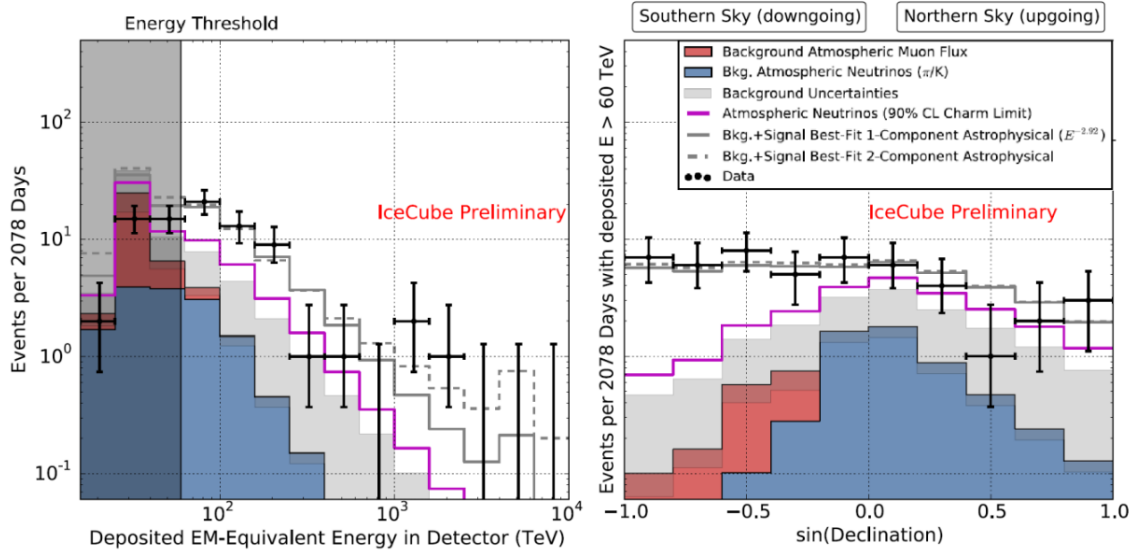


Figure 24: Deposited energies (left) and arrival directions (right) of IceCube HESE events for 6 years of data. The black crosses indicate the data points. The red (blue) region shows the expected background from atmospheric muons (neutrinos) while the grey bar accounts for systematic uncertainties on their sum. The grey lines indicate the total expected number of events including as well the contribution from astrophysical neutrinos.

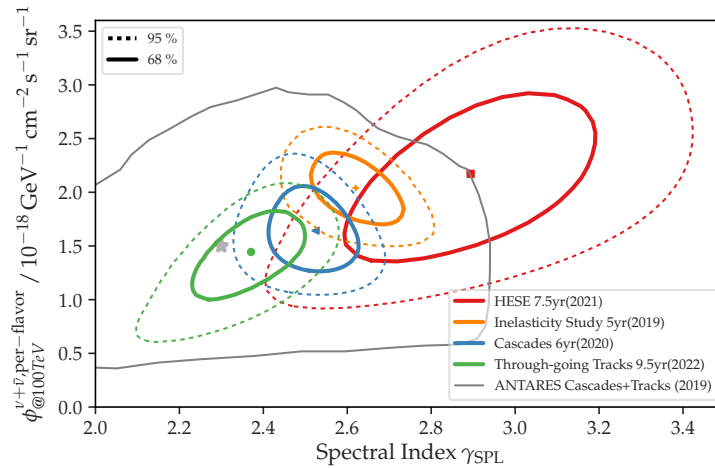


Figure 25: Summary of the recent constraints on the all-sky diffuse astrophysical flux assuming a single power law fluxes. The plain (dotted) lines correspond to 68% (95%) confidence intervals in terms of the spectral index and the per-flavor flux normalization [70].

A similar analysis was performed with the ANTARES detector, using a sample including both track-like and shower-like events. The analysis of the first 8 years of ANTARES resulted in 33 events (19 tracks + 14 showers) in data compared to 24 ± 7 (stat.+syst.) expected background events based on Monte Carlo simulations, leading to a 1.6σ excess compatible with the one observed by IceCube, but not tightly constraining. KM3NeT/ARCA will pursue the efforts, as it is expected to observe the IceCube signal with 3σ (5σ) significance in 3 months (6 months) once the detector is completed (not even considering data taken with partial detector configurations before that).

As can be seen in the right panel of Figure 24, the rates are compatible with a homogeneous distribution in the sky, not showing any preferential arrival direction for neutrinos. The search for localized point sources will be detailed in the next section.

One particular region of interest is the Galactic Plane, an extended region centered on the Milky Way central supermassive black hole and covering the full Galactic Disk. As we have seen in section 2.4.2, it is a likely source of high-energy neutrinos as TeV gamma-rays have been detected from this region and these may have been produced in hadronic processes that would also emit neutrinos.

Recent results from ANTARES [71] and IceCube [72] show the first evidence for such an emission. The latest ANTARES search focuses on a diffuse emission in a limited region around the Galactic Center called the “Galactic Ridge”; it has observed a 2σ excess using both track-like and shower-like events. The observed flux is shown in Figure 26a and it is compatible with the predictions from extrapolation of the gamma-ray observations from Fermi-LAT. As shown in Figure 26b, the most recent publication from IceCube has tested the KRA γ model [73], which tries to reproduce the extended emission over the Galactic Plane, exploiting the gamma-ray measurements to predict the corresponding neutrino emission, both in energy and spatial distribution. The analysis considered high-energy shower-like events and reported a 4.5σ excess in favor of such an emission. The observed galactic neutrino emission accounts for about 10% of the all-sky diffuse neutrino flux [72], and the observations from ANTARES and IceCube are both consistent with the hypothesis of a hadronic origin of the gamma-ray emission observed by Fermi-LAT [74].

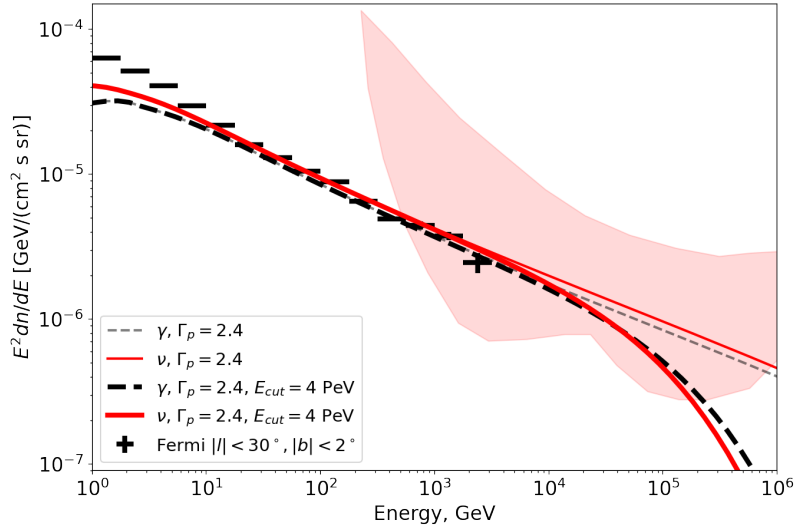
4.2 Search for point sources

The exact origin of the diffuse neutrino flux observed by IceCube since 2013 cannot be determined by the analysis described in the previous section. To identify the underlying sources, it is thus essential to search for neutrino sources, i.e., anisotropies or clusters of neutrinos in the all-sky data.

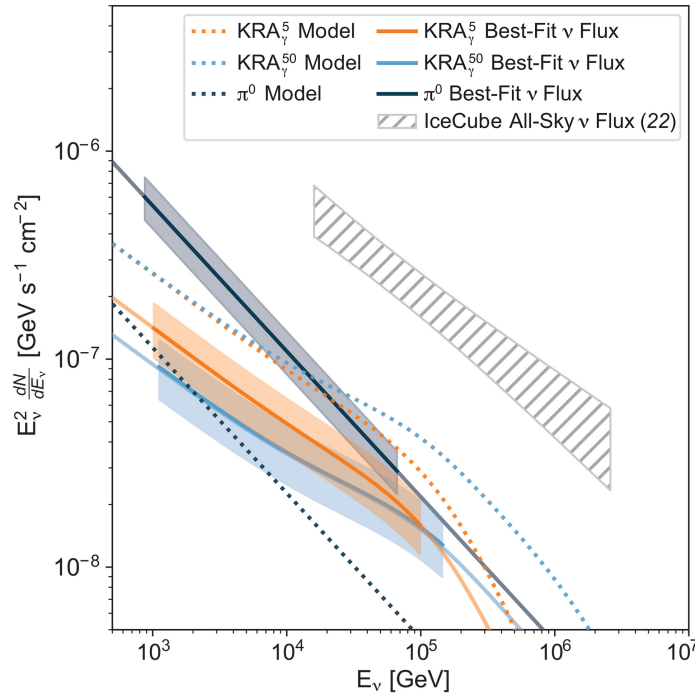
When doing such a study, it is important to correct for the possibility of the signal being just a random statistical fluctuation. This is the meaning of pre- and post-trial significance/p-value. The pre-trial significance is computed directly by looking at the individual observations without correction. The post-trial significance is corrected by computing the chance probability that, by doing many observations (the number of trials is called the trial factor), you end up with a significant source by random fluctuations. An example of such a procedure is described in [75].

Three main approaches may be followed to search for neutrino sources:

- **All-sky search:** the sky is divided into a grid with a finer spacing than the typical reconstruction uncertainty. A Test Statistic (TS) is then evaluated in each bin of the grid and clusters



(a) ANTARES [71] measurement. The red filled region shows the 68% constraint on the diffuse flux from the Galactic Ridge.



(b) IceCube [72] constraints on various template models.

Figure 26: Recent measurements of the Galactic neutrino flux by ANTARES and IceCube. The observed fluxes are compared with models adjusted to the gamma-ray observations (top: simple pion decay model with an injected proton spectrum of spectral index $\Gamma_p = 2.4$ and possible cutoff; bottom: three different templates including the KRA_γ model with different choices for the proton cutoff energy).

with the largest TS are identified as hotspots.

- *Advantage*: unbiased by electromagnetic observations (no prior assumptions regarding directions in the sky).
 - *Disadvantage*: large trial factor, meaning that observed excesses should be penalized because of the important probability of getting such outliers in the background-only hypothesis.
- **Source list search**: the investigated directions are given by the location of selected sources already detected in the electromagnetic spectrum. TS is evaluated for each single source.
 - *Advantage*: reduced trial factor, as we limit the number of directions to be probed with respect to the all-sky search.
 - *Disadvantage*: the search is biased as the brightest neutrino sources may differ from the brightest electromagnetic sources.
 - **Stacking/Population search**: search for an excess from several sources. All the sources in a given catalog are analyzed together (“stacking”) leading to overall constraints on the total signal and on the typical emission from these objects.
 - *Advantage*: sensitive to individually weak sources that produce a significant cumulative signal.
 - *Disadvantage*: the search is biased for the same reason as for the source list searches.

The most significant source, in both all-sky searches and targeted source list searches, in IceCube data is NGC 1068/M77 [76], a Seyfert II galaxy seen with a sensitivity of 2.9σ post-trial (4.1σ pre-trial) when targeted. This observation triggered more detailed studies with all available data, confirming the neutrino emission from the active galaxy with an excess of about 79 neutrinos and a global significance of 4.2σ [77].

The second most significant source identified by IceCube is TXS 0506+056, a blazar observed with a significance of 2.3σ post-trial after the detection of one very-high-energy neutrino by the experiment. This object was also observed through the multi-messenger strategy described in [section 4.3](#) [78]. The source is about 100 times farther away compared to NGC 1068, indicating how bright it has been during the detected flare.

ANTARES has produced similar searches on their data [79], though it does not show any additional significant source. KM3NeT/ARCA has already started to join the efforts. With the complete detector, KM3NeT/ARCA will be able to achieve more than one order of magnitude improvement in the Southern hemisphere with respect to IceCube, as shown in [Figure 27a](#). It will also be able to directly constrain hadronic scenarios in galactic TeV gamma-ray sources ([Figure 27b](#)).

The most promising sources that emerged from these analyses both in IceCube and ANTARES data are AGN and radio galaxies. This has been claimed in different publications by both collaborations [81] as well as by external authors [82].

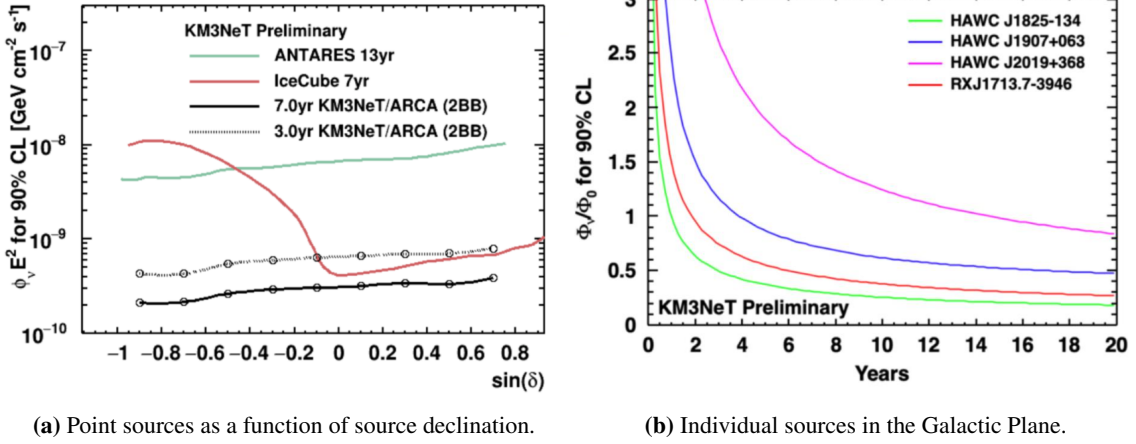


Figure 27: Sensitivity of the complete KM3NeT/ARCA detector to the neutrino flux from point-like sources [80]. The left panel shows comparisons with ANTARES and IceCube; KM3Net is able to outperform IceCube for negative declinations (Southern hemisphere) as, in this region, it can benefit from Earth filtering to reduce the atmospheric muon contamination. The right panel shows how long the detector has to run to detect individual sources in the Galaxy; the horizontal axis corresponds to the number of data-taking years with the KM3NeT/ARCA detector and the vertical axis shows the ratio between the expected sensitivity and the estimated flux based on hadronic models.

4.3 Multi-messenger search

As discussed in section 2.1, neutrinos bring complementary information on the physical processes occurring in astrophysical sources. Therefore, multi-messenger approaches are vital to understand how neutrinos and other messengers are produced, especially for transient phenomena (relatively short bursts where several messengers are emitted in a time scale of a few seconds to a few days). There are two strategies to perform such searches, as described in the two following sections.

4.3.1 Neutrino follow-up of other alerts

When an external alert (from electromagnetic observatories, gravitational wave interferometers, or other neutrino alerts) is received by a neutrino telescope, a search for coincident neutrinos can be performed. This approach has been tested on a broad list of potential sources (e.g. GRBs, microquasar, compact binary mergers, blazar, supernovae, Fast Radio Bursts) with no association so far [83–85]. One of the most promising transient sources was the binary neutron star merger GW170817 detected in gravitational waves by LIGO/Virgo and across the electromagnetic spectrum by many telescopes. However, the search for a coincident signal in ANTARES, IceCube, and Pierre Auger detectors did not lead to a detection [86], as illustrated on Figure 28.

4.4 Follow-up of neutrino alerts

When a very-high-energy neutrino with high astrophysical origin probability is detected by a neutrino telescope, an alert is sent to the community, so that astronomers can perform follow-ups, pointing their instrument in the direction of the detected neutrino. This second approach led to a

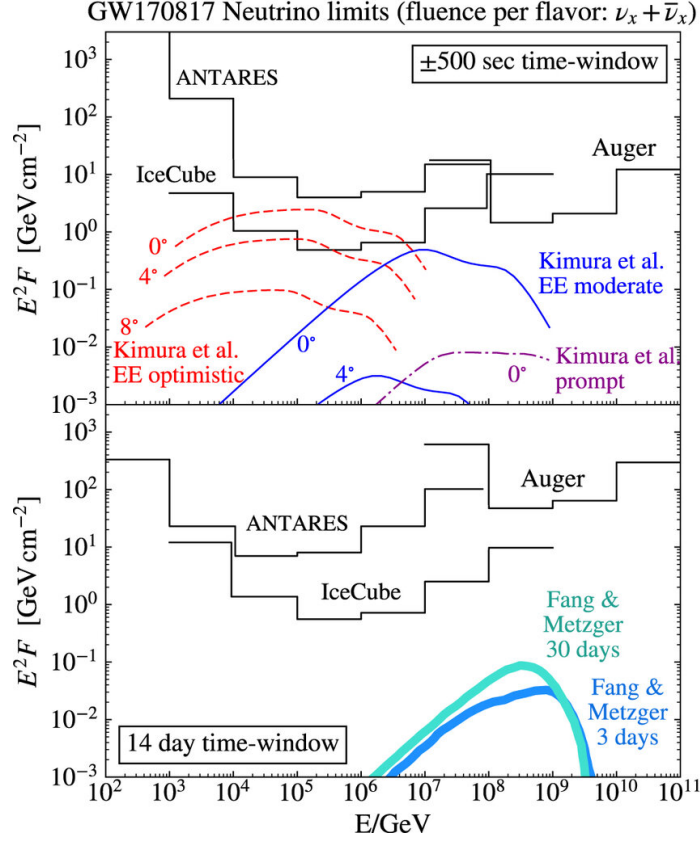


Figure 28: Upper limits on the neutrino spectral fluence from GW170817 for ANTARES, IceCube and Pierre Auger, in a 500 s window around the merger (top) and in a 14 d window after the merger (bottom). Predictions for neutrino emission for prompt emission and extended emission (EE) are shown with colored lines [86].

huge success when, on the 22nd of September, 2017, an electromagnetic follow-up campaign of the event IceCube-170922A indicated that this event came from the direction of a known AGN blazar named TXS 0506+056, a BL Lac object, found at redshift $z = 0.3365 \pm 0.0010$. The AGN was monitored by Fermi-LAT and observed by MAGIC after the IceCube trigger. It was found flaring in multiple wavelengths at the time of the alert, achieving a significance for such a correlation of about 3σ [78].

After the event, further analysis of archival IceCube data revealed that this blazar was emitting neutrinos in the previous years: in a cone of radius 1° centered on the source position, an excess of 13 ± 5 events over the expected background of ~ 6 events was found between October 2014 and March 2015 [87], as shown in Figure 29. The excess had not been identified before because the post-trial significance was lowered below the discovery threshold by the huge amount of trial observations done. As can be seen in the same figure, during that period, there was no significant electromagnetic activity [88], challenging theoretical models.

Blazars are radio-loud AGNs whose relativistic jet points towards the observer. The radiative emission from the jet dominates over all other components leading to a non-thermal spectrum from radio to gamma rays and a fast variability. The multi-messenger observation and the subsequent IceCube archival search have led to a huge theoretical effort to explain the neutrino emission without

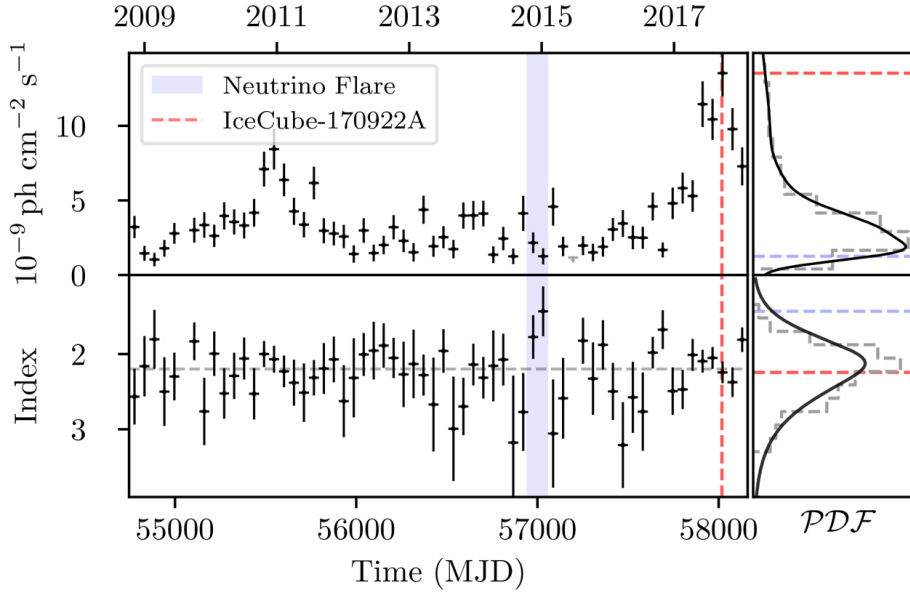
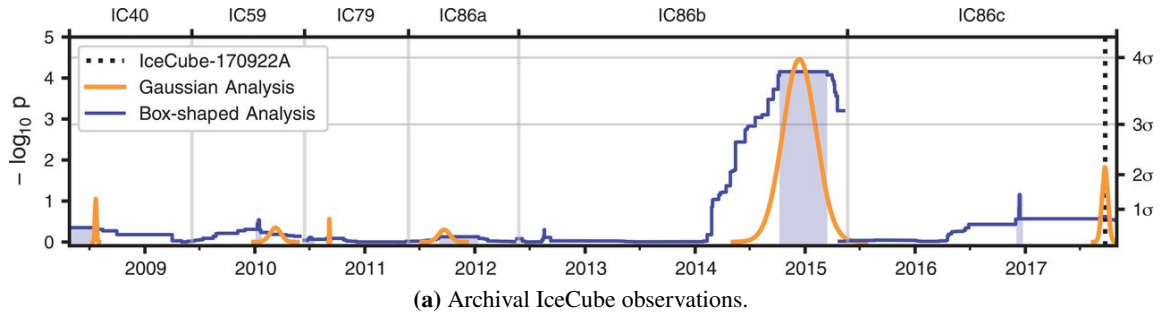


Figure 29: Multi-messenger observations of TXS 0505+056 in the nine years prior to IceCube-170922A.

an electromagnetic flare counterpart [89]. Since the IceCube announcement, other blazars have been monitored as good candidates for neutrino emission, even though no definitive association has been found yet.

In 2019, other observations triggered by IceCube neutrino follow-ups point toward neutrino emission from Tidal Disruption Events [90]. The evidence is however not yet strong enough to draw firm conclusions.

5. Future Prospects

In the near future, the IceCube detector will undergo a series of upgrades, notably the inclusion of seven new strings of multi-PMT optical modules in the DeepCore region. This will be followed by the construction of IceCube-Gen2, an extension of the current observatory, with the main aim of greatly extending the sensitivity to ultra-high-energy neutrinos and eventually detecting EeV cosmogenic neutrinos, as shown in Figure 30. This would be achieved with the inclusion of ~ 120 new strings increasing the volume of the instrument up to 10 km^3 [17].

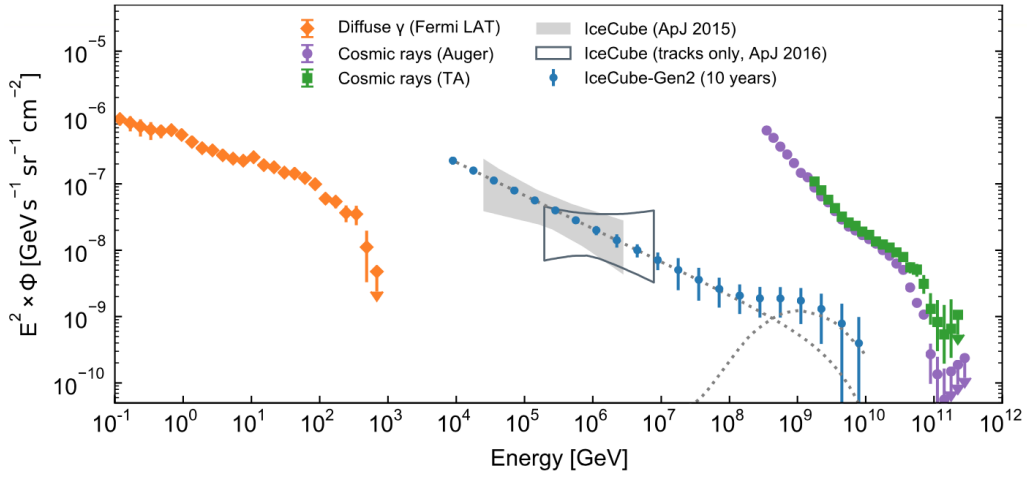


Figure 30: Diffuse neutrino flux observed by IceCube (gray bands) compared with the gamma-ray emission (orange) and UHE cosmic rays (green and violet). Neutrino data are fitted by a single power law (dashed line) and a contribution of cosmogenic neutrinos is also expected at EeV energies. The expected flux measurements with 10 years of IceCube-Gen2 are illustrated with blue points [17].

In parallel, the KM3NeT experiment is currently under construction, as already described in section 3.2. The first lines have been deployed and are taking data, such that preliminary results have started to be produced by the collaboration. The instantaneous acceptance of the KM3NeT detector already exceeds the ANTARES one, such that it already provides more constraining limits on the neutrino flux from transient phenomena. In the coming years, it will also outperform the diffuse and point-source searches performed by ANTARES. With its two sites having complementary energy coverage, the KM3NeT experiment will not only have the possibility of carrying out astrophysical studies but will also be able to directly probe the relative ordering of neutrino masses (mass hierarchy) [91].

The Baikal Collaboration has also made great progress in constructing a kilometer-scale detector in Lake Baikal called GVD (for Giga-ton Volume detector) [92].

The existence of a diffuse flux of astrophysical neutrinos is firmly confirmed and a few sources have recently been discovered. With current and future instruments, we expect to unveil more neutrino sources including objects observed simultaneously with several messengers, therefore improving our understanding of underlying production mechanisms.

References

- [1] S.M. Bilenky and C. Giunti, *Neutrinoless Double-Beta Decay: a Probe of Physics Beyond the Standard Model*, *Int. J. Mod. Phys. A* **30** (2015) 1530001 [1411.4791].
- [2] M. Fukugita and T. Yanagida, *Baryon asymmetry in the universe and neutrinos*, in *Physics of Neutrinos: and Application to Astrophysics*, (Berlin, Heidelberg), pp. 487–516, Springer Berlin Heidelberg (2003), DOI.
- [3] PARTICLE DATA GROUP collaboration, *Review of Particle Physics*, *PTEP* **2022** (2022) 083C01.
- [4] A. Franklin, *Are there really neutrinos? An evidential history*, *Frontiers in Physics* (11, 2000).
- [5] E. Fermi, *Versuch einer Theorie der β -Strahlen. I*, *Zeitschrift für Physik* **88** (1934) 161.
- [6] P. Ramond, *Neutrinos and Particle Physics Models*, in *International Conference on History of the Neutrino: 1930-2018*, 2, 2019 [1902.01741].
- [7] J. Rohlf, *Modern Physics from alpha to Z0*, Wiley (1994).
- [8] T.D. Lee and C.N. Yang, *Question of Parity Conservation in Weak Interactions*, *Physical Review* **104** (1956) 254.
- [9] C.S. Wu, E. Ambler, R.W. Hayward, D.D. Hoppes and R.P. Hudson, *Experimental test of parity conservation in beta decay*, *Phys. Rev.* **105** (1957) 1413.
- [10] M. Goldhaber, L. Grodzins and A.W. Sunyar, *Helicity of Neutrinos*, *Physical Review* **109** (1958) 1015.
- [11] K. Zuber, *Neutrino Physics*, Taylor & Francis, Boca Raton (2020), 10.1201/9781315195612.
- [12] G. Danby, J.-M. Gaillard, K. Goulianos, L.M. Lederman, N. Mistry, M. Schwartz et al., *Observation of high-energy neutrino reactions and the existence of two kinds of neutrinos*, *Phys. Rev. Lett.* **9** (1962) 36.
- [13] G.S. Abrams and others., *Searches for new quarks and leptons produced in z-boson decay*, *Phys. Rev. Lett.* **63** (1989) 2447.
- [14] DONUT collaboration, *Observation of tau neutrino interactions*, *Phys. Lett. B* **504** (2001) 218 [hep-ex/0012035].
- [15] J.A. Formaggio and G.P. Zeller, *From eV to EeV: Neutrino Cross Sections Across Energy Scales*, *Rev. Mod. Phys.* **84** (2012) 1307 [1305.7513].
- [16] T. Chiarusi and M. Spurio, *High-energy astrophysics with neutrino telescopes*, *The European Physical Journal C* **65** (2010) 649.

- [17] M.G. Aartsen et al., *IceCube-Gen2: the window to the extreme Universe*, *Journal of Physics G Nuclear Physics* **48** (2021) 060501 [2008.04323].
- [18] F. Reines, *Neutrino Interactions*, *Annual Review of Nuclear and Particle Science* **10** (1960) 1.
- [19] K. Greisen, *Cosmic Ray Showers*, *Annual Review of Nuclear and Particle Science* **10** (1960) 63.
- [20] D. D'Angelo et al., *Recent Borexino results and prospects for the near future*, in *European Physical Journal Web of Conferences*, vol. 126 of *European Physical Journal Web of Conferences*, p. 02008, Nov., 2016, DOI.
- [21] B.T. Cleveland, T. Daily, J. Davis, Raymond, J.R. Distel, K. Lande, C.K. Lee et al., *Measurement of the Solar Electron Neutrino Flux with the Homestake Chlorine Detector*, *ApJ* **496** (1998) 505.
- [22] Y. Fukuda et al., *Measurements of the solar neutrino flux from super-kamiokande's first 300 days*, *Phys. Rev. Lett.* **81** (1998) 1158.
- [23] "The Nobel Prize in Physics 2002." [Press release](#).
- [24] SNO collaboration, *Measurement of the rate of $\nu_e + d \rightarrow p + p + e^-$ interactions produced by ^8B solar neutrinos at the Sudbury Neutrino Observatory*, *Phys. Rev. Lett.* **87** (2001) 071301 [nucl-ex/0106015].
- [25] SUPER-KAMIOKANDE collaboration, *Evidence for oscillation of atmospheric neutrinos*, *Phys. Rev. Lett.* **81** (1998) 1562 [hep-ex/9807003].
- [26] SUPER-KAMIOKANDE collaboration, *Evidence for oscillation of atmospheric neutrinos*, *Phys. Rev. Lett.* **81** (1998) 1562.
- [27] SUPER-KAMIOKANDE collaboration, *Measurement of atmospheric neutrino oscillation parameters by Super-Kamiokande I*, *Phys. Rev. D* **71** (2005) 112005.
- [28] Q.R. Ahmad et al., *Measurement of the Rate of $\nu_e + d \rightarrow p + p + e^-$ Interactions Produced by ^8B Solar Neutrinos at the Sudbury Neutrino Observatory*, *Phys. Rev. Lett.* **87** (2001) 071301 [nucl-ex/0106015].
- [29] Q.R. Ahmad et al., *Direct Evidence for Neutrino Flavor Transformation from Neutral-Current Interactions in the Sudbury Neutrino Observatory*, *Phys. Rev. Lett.* **89** (2002) 011301 [nucl-ex/0204008].
- [30] E. Fermi, *On the Origin of the Cosmic Radiation*, *Phys. Rev.* **75** (1949) 1169.
- [31] P. Padovani et al., *Active galactic nuclei: what's in a name?*, *Astron. Astrophys. Rev.* **25** (2017) 2 [1707.07134].
- [32] F.W. Stecker, C. Done, M.H. Salamon and P. Sommers, *High-energy neutrinos from active galactic nuclei*, *Phys. Rev. Lett.* **66** (1991) 2697.

- [33] B. Zhang, *The Physics of Gamma-Ray Bursts*, Cambridge University Press (12, 2018).
- [34] E. Waxman and J.N. Bahcall, *High-energy neutrinos from cosmological gamma-ray burst fireballs*, *Phys. Rev. Lett.* **78** (1997) 2292 [astro-ph/9701231].
- [35] L.J. Kewley, M.A. Dopita, R.S. Sutherland, C.A. Heisler and J. Trevena, *Theoretical modeling of starburst galaxies*, *Astrophys. J.* **556** (2001) 121 [astro-ph/0106324].
- [36] E. Peretti, P. Blasi, F. Aharonian, G. Morlino and P. Cristofari, *Contribution of starburst nuclei to the diffuse gamma-ray and neutrino flux*, *Mon. Not. Roy. Astron. Soc.* **493** (2020) 5880 [1911.06163].
- [37] S. Gezari, *Tidal Disruption Events*, *Ann. Rev. Astron. Astrophys.* **59** (2021) 21 [2104.14580].
- [38] J.M. Cordes and S. Chatterjee, *Fast Radio Bursts: An Extragalactic Enigma*, *Ann. Rev. Astron. Astrophys.* **57** (2019) 417 [1906.05878].
- [39] K. Nishiwaki, K. Asano and K. Murase, *High-energy Neutrino Constraints on Cosmic-Ray Reacceleration in Radio Halos of Massive Galaxy Clusters*, *Astrophys. J.* **954** (2023) 188 [2307.13273].
- [40] FERMI-LAT collaboration, *Fermi-LAT Observations of the Diffuse Gamma-Ray Emission: Implications for Cosmic Rays and the Interstellar Medium*, *Astrophys. J.* **750** (2012) 3 [1202.4039].
- [41] FERMI-LAT collaboration, *Detection of the Characteristic Pion-Decay Signature in Supernova Remnants*, *Science* **339** (2013) 807 [1302.3307].
- [42] L.A. Anchordoqui, D.F. Torres, T.P. McCauley, G.E. Romero and F.A. Aharonian, *Neutrinos from accreting neutron stars*, *Astrophys. J.* **589** (2003) 481 [hep-ph/0211231].
- [43] ANTARES collaboration, *A Search for Time Dependent Neutrino Emission from Microquasars with the ANTARES Telescope*, *JHEAp* **3-4** (2014) 9 [1402.1600].
- [44] C. Thompson and R.C. Duncan, *The Soft gamma repeaters as very strongly magnetized neutron stars. 2. Quiescent neutrino, x-ray, and Alfvén wave emission*, *Astrophys. J.* **473** (1996) 322.
- [45] ICECUBE collaboration, *Searches for Time Dependent Neutrino Sources with IceCube Data from 2008 to 2012*, *Astrophys. J.* **807** (2015) 46 [1503.00598].
- [46] P.A. Cherenkov, *Visible emission of clean liquids by action of γ radiation*, *Doklady Akademii nauk SSSR* **2** (1934) 451.
- [47] M.A. Markov and I.M. Zheleznykh, *On high energy neutrino physics in cosmic rays*, *Nuclear Physics* **27** (1961) 385.
- [48] F. Bernard, *Caractérisation Des Performances D'un Telescope Sous-marin A Neutrinos Pour La Detection De Cascades Contenues Dans Le Cadre Du Projet Antares*, Ph.D. thesis, Marseille, CPPM, 2000.

- [49] M. Ackermann et al., *Optical properties of deep glacial ice at the South Pole*, *J. Geophys. Res.* **111** (2006) D13203.
- [50] F. Halzen, *High-energy neutrino astrophysics*, *Nature Physics* **13** (2017) 232.
- [51] J.A. Aguilar et al., *A fast algorithm for muon track reconstruction and its application to the ANTARES neutrino telescope*, *Astroparticle Physics* **34** (2011) 652 [1105.4116].
- [52] T. Chiarusi and M. Spurio, *High-energy astrophysics with neutrino telescopes*, *European Physical Journal C* **65** (2010) 649 [0906.2634].
- [53] K.K. Young, *DUMAND-II (deep underwater muon and neutrino detector) progress report*, in *Intersections between Particle and Nuclear Physics*, S.J. Seestrom, ed., vol. 338 of *American Institute of Physics Conference Series*, pp. 886–892, July, 1995, DOI [astro-ph/9412060].
- [54] AMANDA collaboration, *Status of AMANDA neutrino observatory*, in *International Workshop on Simulations and Analysis Methods for Large Neutrino Telescopes*, pp. 47–60, 1998.
- [55] ICECUBE collaboration, *The IceCube Neutrino Observatory: Instrumentation and Online Systems*, *JINST* **12** (2017) P03012 [1612.05093].
- [56] ICECUBE collaboration, *First Observation of PeV-Energy Neutrinos with IceCube*, *Phys. Rev. Lett.* **111** (2013) 021103.
- [57] ICECUBE collaboration, *Evidence for High-Energy Extraterrestrial Neutrinos at the IceCube Detector*, *Science* **342** (2013) 1242856 [1311.5238].
- [58] ICECUBE collaboration, *Observation of High-Energy Astrophysical Neutrinos in Three Years of IceCube Data*, *Phys. Rev. Lett.* **113** (2014) 101101.
- [59] ICECUBE collaboration, *IceCube high-energy starting event sample: Description and flux characterization with 7.5 years of data*, *Phys. Rev. D* **104** (2021) 022002.
- [60] ANTARES collaboration, *ANTARES: the first undersea neutrino telescope*, *Nucl. Instrum. Meth. A* **656** (2011) 11 [1104.1607].
- [61] KM3NET collaboration, *Letter of intent for KM3NeT 2.0*, *J. Phys. G* **43** (2016) 084001 [1601.07459].
- [62] KM3NET collaboration, *Contributions of KM3NeT to ICRC2023*, in *38th International Cosmic Ray Conference*, 9, 2023 [2309.05016].
- [63] A. Albert et al., *The cosmic ray shadow of the Moon observed with the ANTARES neutrino telescope*, *European Physical Journal C* **78** (2018) 1006 [1807.11815].
- [64] ANTARES collaboration, *Observation of the cosmic ray shadow of the Sun with the ANTARES neutrino telescope*, *Phys. Rev. D* **102** (2020) 122007.

- [65] X. Durrieu de Madron, S. Ramondenc, L. Berline, L. Houpert, A. Bosse, S. Martini et al., *Deep sediment resuspension and thick nepheloid layer generation by open-ocean convection*, *Journal of Geophysical Research: Oceans* **122** (2017) 2291.
- [66] H. Haren, S. Adrián-Martínez, I. Al Samarai, A. Albert, M. André, M. Anghinolfi et al., *High-frequency internal wave motions at the ANTARES site in the deep Western Mediterranean*, *Ocean Dynamics* **64** (2014) pages 507–517.
- [67] C. Tamburini, M. Canals, X. Durrieu de Madron, L. Houpert, D. Lefevre, s. Martini et al., *Deep-Sea Bioluminescence Blooms after Dense Water Formation at the Ocean Surface*, *PLoS one* **8** (2013) e67523.
- [68] K. Greisen, *End to the cosmic-ray spectrum?*, *Phys. Rev. Lett.* **16** (1966) 748.
- [69] G.T. Zatsepin and V.A. Kuz'min, *Upper Limit of the Spectrum of Cosmic Rays*, *Soviet Journal of Experimental and Theoretical Physics Letters* **4** (1966) 78.
- [70] M. Ackermann et al., *High-energy and ultra-high-energy neutrinos: A Snowmass white paper*, *JHEAp* **36** (2022) 55 [2203.08096].
- [71] ANTARES collaboration, *Hint for a TeV neutrino emission from the Galactic Ridge with ANTARES*, *Phys. Lett. B* **841** (2023) 137951 [2212.11876].
- [72] ICECUBE collaboration, *Observation of high-energy neutrinos from the Galactic plane*, *Science* **380** (2023) adc9818 [2307.04427].
- [73] D. Gaggero, D. Grasso, A. Marinelli, A. Urbano and M. Valli, *The gamma-ray and neutrino sky: A consistent picture of Fermi-LAT, Milagro, and IceCube results*, *Astrophys. J. Lett.* **815** (2015) L25 [1504.00227].
- [74] A. Neronov, D. Semikoz, J. Aublin, M. Lamoureux and A. Kouchner, *Hadronic nature of high-energy emission from the Galactic Ridge*, 2307.07978.
- [75] ANTARES collaboration, *ANTARES Search for Point Sources of Neutrinos Using Astrophysical Catalogs: A Likelihood Analysis*, *Astrophys. J.* **911** (2021) 48 [2012.15082].
- [76] M.G. Aartsen et al., *Time-Integrated Neutrino Source Searches with 10 Years of IceCube Data*, *Phys. Rev. Lett.* **124** (2020) 051103.
- [77] ICECUBE collaboration, *Evidence for neutrino emission from the nearby active galaxy NGC 1068*, *Science* **378** (2022) 538 [2211.09972].
- [78] M.G. Aartsen et al., *Multimessenger observations of a flaring blazar coincident with high-energy neutrino IceCube-170922A*, *Science* **361** (2018) eaat1378 [1807.08816].
- [79] A. Albert et al., *ANTARES and IceCube Combined Search for Neutrino Point-like and Extended Sources in the Southern Sky*, *ApJ* **892** (2020) 92 [2001.04412].

- [80] S. Celli, *KM3NeT: status and perspectives for neutrino astronomy from the MeV to the PeV*, in *Journal of Physics Conference Series*, vol. 2156 of *Journal of Physics Conference Series*, p. 012105, Dec., 2021, DOI.
- [81] A. Plavin, Y.Y. Kovalev, Y.A. Kovalev and S. Troitsky, *Observational Evidence for the Origin of High-energy Neutrinos in Parsec-scale Nuclei of Radio-bright Active Galaxies*, *ApJ* **894** (2020) 101 [2001.00930].
- [82] S. Buson, A. Tramacere, L. Pfeiffer, L. Oswald, R. de Menezes, A. Azzollini et al., *Beginning a Journey Across the Universe: The Discovery of Extragalactic Neutrino Factories*, *ApJ* **933** (2022) L43 [2207.06314].
- [83] ICECUBE collaboration, *Extending the Search for Muon Neutrinos Coincident with Gamma-Ray Bursts in IceCube Data*, *ApJ* **843** (2017) 112 [1702.06868].
- [84] ANTARES collaboration, *Search for high-energy neutrinos from bright GRBs with ANTARES*, *MNRAS* **469** (2017) 906 [1612.08589].
- [85] ANTARES collaboration, *Constraining the contribution of Gamma-Ray Bursts to the high-energy diffuse neutrino flux with 10 yr of ANTARES data*, *MNRAS* **500** (2021) 5614 [2008.02127].
- [86] A. Albert et al., *Search for High-energy Neutrinos from Binary Neutron Star Merger GW170817 with ANTARES, IceCube, and the Pierre Auger Observatory*, *ApJ* **850** (2017) L35 [1710.05839].
- [87] ICECUBE collaboration, *Neutrino emission from the direction of the blazar TXS 0506+056 prior to the IceCube-170922A alert*, *Science* **361** (2018) 147 [1807.08794].
- [88] P. Padovani, P. Giommi, E. Resconi, T. Glauch, B. Arsioli, N. Sahakyan et al., *Dissecting the region around IceCube-170922A: the blazar TXS 0506+056 as the first cosmic neutrino source*, *MNRAS* **480** (2018) 192 [1807.04461].
- [89] P. Padovani, P. Giommi, E. Resconi, T. Glauch, B. Arsioli, N. Sahakyan et al., *Dissecting the region around IceCube-170922A: the blazar TXS 0506+056 as the first cosmic neutrino source*, *Mon. Not. Roy. Astron. Soc.* **480** (2018) 192 [1807.04461].
- [90] R. Stein et al., *A tidal disruption event coincident with a high-energy neutrino*, *Nature Astron.* **5** (2021) 510 [2005.05340].
- [91] KM3NET collaboration, *Particle Physics with ORCA*, *EPJ Web Conf.* **207** (2019) 04003.
- [92] BAIKAL-GVD collaboration, *Baikal-GVD: status and prospects*, *EPJ Web Conf.* **191** (2018) 01006 [1808.10353].